Comparative techno-economic and life cycle greenhouse gas assessment of ammonia production from thermal decomposition of methane and steam methane reforming technologies

A.O. Oni[a,1], T. Giwa[b], C. Font-Palma[c], D.A. Fadare[d]

[a]Department of Mechanical Engineering, 10-263 Donadeo Innovation Centre for Engineering, University of Alberta, Edmonton, Alberta T6G 1H9, Canada

[b]Department of Mechanical Engineering, Federal University of Agriculture, Abeokuta, P.M.B. 2240, Abeokuta, Ogun State, Nigeria

[c]School of Engineering, University of Hull, HU6 7RX, United Kingdom

[d]Department of Mechanical Engineering, University of Ibadan, P.M.B. 1, Ibadan, Nigeria

Abstract

This study assesses the life cycle greenhouse gas (GHG) and economic feasibility of applying thermal decomposition of methane (TDM) technology for ammonia production compared to the conventional steam methane reforming (SMR) technology. A detailed process model for each ammonia-based technology was developed to get data to perform energy, life cycle GHG emissions, and economic analyses. The results showed that the SMR plant consumes 30.3% more fuel than the TDM. The life cycle GHG emissions of TDM and SMR are 1.42 and 2.51 t CO_2e/t NH_3, respectively. The combustion and process emissions released to the environment and electricity emissions take a large share in the life cycle emissions of SMR and TDM, respectively. The production cost of ammonia from SMR is lower than TDM by \$69/t NH_3. TDM requires a higher investment because of high capital costs and the huge amount of natural gas needed as feedstock. For TDM, the sale of the oxygen product does not provide sufficient revenue to outperform

[1] Corresponding author
E-mail: fem2day@yahoo.com (A.O. Oni).

SMR. Integrating a carbon capture unit into TDM improves its economic performance, and it does not require revenue from the sales of an oxygen product to outperform SMR with a carbon capture unit. The results also showed that SMR (without carbon capture and storage) is more economically attractive when the carbon price benchmark is below \$99/t CO_2. Above this carbon price, integrating a carbon capture unit into TDM is economically preferable.

Keywords: Thermal decomposition of methane; Steam methane reforming; Ammonia; life cycle greenhouse gas; production cost

1. Introduction

Ammonia is one of the most valuable chemicals in the world. It is produced through the combination of hydrogen and nitrogen under high temperature and pressure. A large portion of the ammonia produced is used for manufacturing fertilizers. The remaining is used for pharmaceuticals, water purification, refrigeration, explosives, cleaning products, etc. The global production capacity was estimated to be over 175 million tonnes in 2016 [1] and is expected to increase by 23% from 2019 to 2030 [2]. Though the use of ammonia is essential, a significant amount of greenhouse gas (GHG) emissions comes from the currently used methods for manufacturing ammonia. The annual fossil fuel use is about 2% of global consumption, which corresponds to CO_2 emissions of over 420 million tonnes per year [3, 4]. To meet the growing demand for ammonia, GHG emissions associated with its production will increase by the same order of magnitude. Thus, developing alternative environmentally friendly production pathways will help to move towards sustainable ammonia plant operations.

Over the years, the development of ammonia production plants has received significant attention. The first large-scale production, a 30-metric tonne per day capacity Haber-Bosch process plant, was commercialized in 1913 [5]. This technology has undergone many modifications, which enabled an increase in efficiency and larger production capacities (up to 3,300 metric tonnes per day). Today, the Haber-Bosch process is popular, well established, and with a technology readiness level (TRL) of 9 [6]. Most of the currently used ammonia technology follows a similar design scheme. The hydrogen needed for ammonia synthesis is produced either by the steam reforming of hydrocarbons or gasification of carbon-based components, such as coal. Depending on the method of hydrogen production, nitrogen is either produced from a secondary reformer by introducing air (or oxygen-enriched air) or from an air separation unit. The hydrocarbon-based processes are widespread, especially the steam reforming of natural gas (about 72%). These processes accounted for 78%, while coal gasification accounts for 22% [7, 8]. Steam reforming of natural gas is popular in North America and most parts of the world except China. It is currently the least energy-intensive method [7]. Its energy consumption ranges from 28 to 33.8 gigajoules of natural gas per tonne of ammonia, and about 1.6 tonnes of CO_2 per tonne of ammonia are released directly into the environment [7, 9]. The

life cycle greenhouse gas emission is about 2.6 tonnes of CO_2 per tonne of ammonia [10]. For comparison, the life cycle GHG emissions of the coal gasification process range from 5.1-7.8 tonne of CO_2 per tonne of ammonia [10, 11], while the energy consumption ranges from 51.3-77 gigajoules per tonne of ammonia [11, 12]. Because of the growing interest in low energy consumption and strict environmental regulations, many plant operators have begun to consider a cleaner pathway. Many of the proposed alternative technologies for GHG emissions reduction are available in the public domain. Most of these technologies produce hydrogen through nuclear, hydropower, municipal waste, biomass, solar, and wind energy. While these technologies are promising, they often come with difficult challenges. Some are costly to implement. Zhang et al. [13] assessed the economic potential of green ammonia production processes using green hydrogen. They studied biomass gasification and water electrolysis for a large-scale ammonia process. Their results showed that while the electrolysis-based process is not economically feasible, the biomass gasification-based process will require a long payback period compared to the conventional steam-methane reforming. Some of these technologies are more complex than the steam-methane reforming process, thus, they increase the uncertainty of plant operations. A nuclear CuCl cycle for ammonia production is a typical example, it involves a multiple-step thermochemical cycle to produce hydrogen [14]. The availability and pre-processing of feedstock, such as biomass and municipal waste, present a potential challenge. Biomass yield depends on adequate economic and environmental conditions [15]. Undesirable environmental conditions could negatively impact biomass yield throughout the year [16]. The wide variability in the composition of feedstocks also presents another challenge. Municipal waste and biomass combustion often result in the release of harmful air pollutants such as carbon monoxide, nitrogen oxides, and volatile organic compounds [17, 18].

Thermal decomposition of methane (TDM) is considered a potentially viable process for the efficient production of hydrogen, currently at TRL 4–5. In this novel process, methane decomposes into its components, carbon and hydrogen, at a high temperature. Because the process is endothermic, methane is passed over a catalyst to lower the reactor temperature and energy consumption. Unlike biomass and

88 municipal waste combustion, the TDM technology produces less harmful pollutants. The process provides
89 the opportunity to lower GHG emissions and reduces the energy intensity of the carbon capture process. It
90 could serve as a solution to a sustainable hydrogen economy [19]. There are several works done on the
91 TDM technology. Abanades investigated the deployment of a TDM technology into a hydrogen economy
92 in the power and mobility sector [20]. Abanades proposes a scheme to deliver hydrogen in a hydrogen-
93 based station into vehicles and a combined power plant. His results showed that the TDM technology lowers
94 greenhouse gas emissions and is economically feasible for both sectors. Keipi et al. [21] evaluated the
95 economic and CO_2 reduction performance of four methane decomposition pathways. The best pathway
96 produces 17% less carbon emission when compared to the reference case (direct methane combustion).
97 They also found that selling carbon has a significant impact on the economy of methane decomposition
98 processes. In another study by Keipi et al. [22], they compared the economic viability of the hydrogen
99 produced from methane decomposition to water electrolysis and steam methane reforming. The results
100 suggest that the thermal decomposition of methane produces fewer emissions and could be economically
101 viable on a small or medium industrial scale. Some studies applied the TDM technology to produce steam
102 for oil sands extraction and hydrotreating intermediates in bitumen upgraders [23, 24].
103 Producing ammonia through the TDM technology will require a nitrogen production unit and a
104 conventional ammonia synthesis reactor. Ultimately, the use of TDM to lower GHG emissions will come
105 at a price. Although earlier works provided insights into the TDM technology, there are currently no studies
106 on carbon footprint and the economic impact of the TDM technology on ammonia production. Furthermore,
107 to the best of our knowledge, this is the first study assessing the integration of TDM technology into
108 ammonia production. In this study, to produce ammonia, we developed TDM and ASU processes and
109 integrated them into an ammonia synthesis reactor. This work aims to assess the carbon footprint and
110 economic viability of applying TDM technology to ammonia production.
111 The objectives of this study are to:
112 • Develop process models for ammonia production through thermal decomposition of methane and
113 steam methane reforming technologies.

- Evaluate the life cycle greenhouse gas emissions and the production cost of ammonia from these technologies.
- Compare the thermal decomposition of methane and steam methane reforming technologies.

2. Method

This study aims to determine whether there are environmental and economic benefits of producing ammonia hydrogen using the TDM technology in Alberta, Canada. Ammonia production requires both hydrogen and nitrogen. The TDM technology produces the needed hydrogen by decomposing natural gas in three reactors in series over an iron oxide catalyst. An air separation unit (ASU) is included to produce the nitrogen needed to synthesize hydrogen for ammonia production. The ammonia-steam reforming process was developed following a typical ammonia industrial plant provided in ref. [25, 26]. MEA was chosen as the solvent for CO_2 capture because of its high absorption rate, relatively low regeneration heat, and low cost [27, 28]. The recovery of CO_2 from flue gas power plants, furnaces, and boilers has been proven to be feasible using the MEA technology [29]. Besides, MEA is still considered the benchmark solvent for carbon capture, particularly in post-combustion processes [30]. This study used the MEA to capture CO_2, leaving the reactors and the furnaces (flue gases). The production capacity of each technology is 2,215 tonnes of ammonia per day.

2.1 Process description

2.1.1 Ammonia production from the steam methane reforming pathway

Fig. 1 presents the schematic diagram of the steam methane reforming (SMR) pathway for ammonia production. Natural gas and steam, at a steam-to-carbon ratio of 3:1, are fed to the primary reformer. The mixture enters the primary reformer at 530^{o}C. The reactions in the reformer take place in its tubes. Because the reactions occurring in the primary reformer are endothermic, fuel (natural gas) is required to raise the operating temperature depending on the steam-to-carbon ratio. Fuel consumption is often optimized by increasing the steam-to-carbon ratio to lower operating temperature [31]. The heat from hot flue gas leaving

the reformer is recovered using the reformer's feed streams (steam and natural gas). The product stream, which is the reformed gas, exits the primary reformer at 830^{o}C. The volume of methane in the exiting stream is regulated to ensure no oxidants leave the secondary reformer. The reformed gas and preheated air enter the secondary reformer as reactants. These reactants burn to produce heat for the endothermic reaction occurring in the secondary reformer. The gas exiting the secondary reformer is at a high temperature. The gas temperature is lowered by heat recovery before being fed into the high and low temperature water-gas-shift (WGS) reactors. In the WGS reactors, the carbon monoxide produced in the primary and secondary reformer reacts with steam over a catalyst to produce hydrogen. The reactions in the WGS reactors are exothermic. The gas stream leaving the WGS flows to the purification unit, where it is cooled to remove water and carbon dioxide. The purification unit comprises separators, monoethanolamine (MEA) scrubbers, a regenerator, and a methanation unit. While water is removed from the gases using the separators, carbon dioxide is scrubbed with MEA solution in an absorber. The carbon dioxide-rich MEA solution from the absorber flows to a regenerator, where the MEA solution is recovered by stripping with steam. The hydrogen-nitrogen-rich gas exiting the absorber is sent to the methanation, where traces of carbon oxides are converted to methane over nickel alumina catalyst. The produced gas is compressed and sent to a 3-bed quench reactor for ammonia production. The product gas contains unconverted feed streams that must be recycled. For this reason, it is cooled in a refrigeration system to liquefy the ammonia. The unconverted gaseous feed is separated and recycled through a high-pressure separator. The liquid product, rich in ammonia, is flashed in a medium pressure separator to remove purge gas.

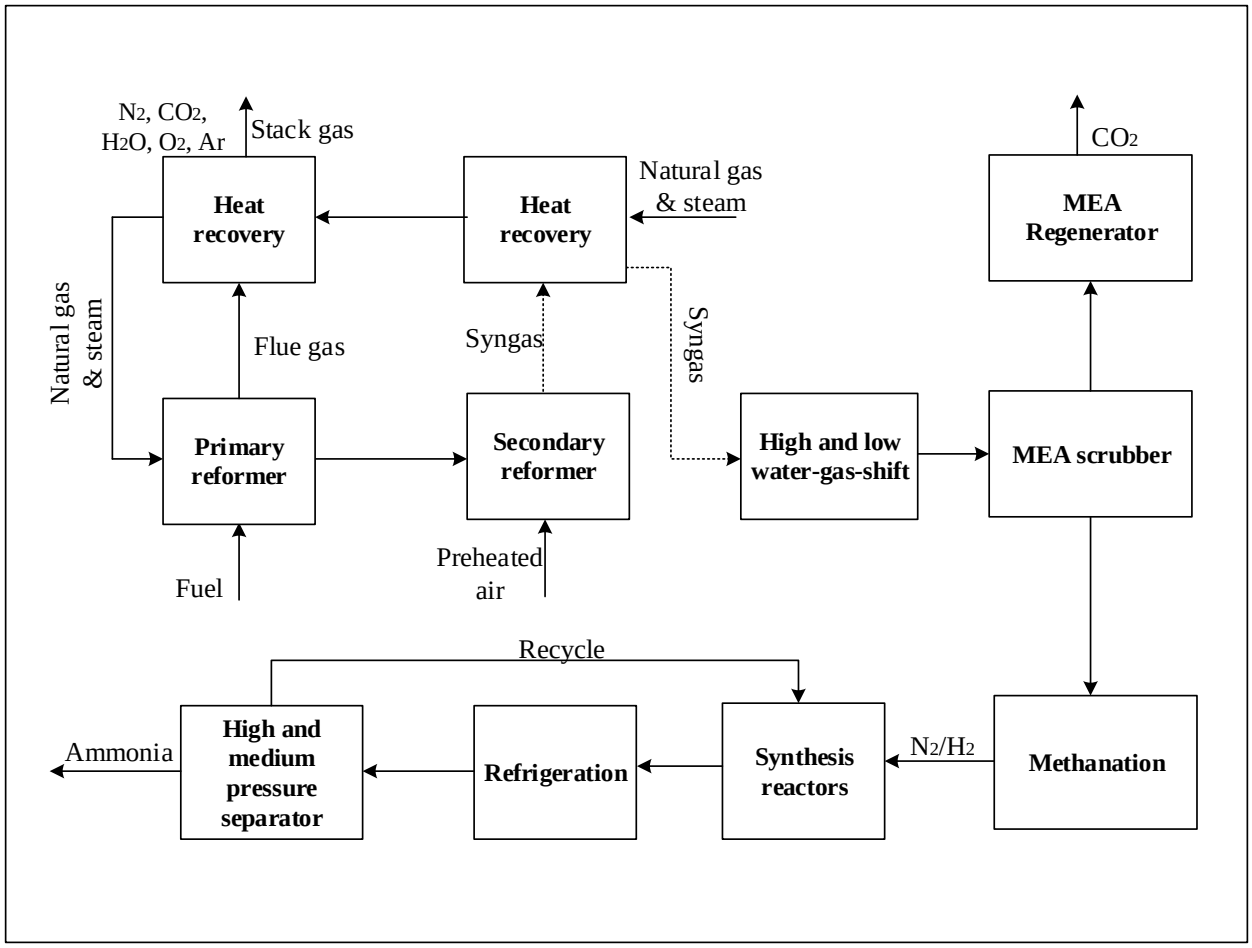

158

159 Fig. 1: Schematic diagram of ammonia production through the SMR pathway

160

2.1.2 Ammonia production from the natural gas thermal decomposition pathway

Fig. 2 presents the TDM pathway to ammonia production. The process has four sections, the decarbonization unit, pressure swing adsorption (PSA) unit, ASU, and ammonia synthesis unit. Hydrogen, nitrogen, and ammonia are produced in the decarbonization unit, ASU, and ammonia synthesis unit, respectively. The ammonia synthesis unit has been described in section 2.1 therefore, it is not repeated here.

Thermal decomposition of methane (TDM) and pressure swing adsorption (PSA) units

The TDM reactors comprise three fluidized bed reactors operating at varying pressures to maximize natural gas conversion to hydrogen and carbon. The reactors are in series, a high-pressure reactor (HPR), a medium-pressure reactor (MPR), and a low-pressure reactor (LPR). These reactors are loaded with low-grade iron oxide catalysts and heated to a high temperature (above 850^{o}C). The feedstock, natural gas, is preheated using the LPR output stream and flue gases at the radiant zone of the reactors' furnaces. The preheated natural gas flows to the HPR reactor, where the reaction starts. The product stream from each reactor (except LPR) is fed to the next to improve natural gas conversion. The conversion ends in LPR. The product leaving each reactor contains mixtures of solid carbon and gases. The mixture of carbon and iron catalyst is separated using cyclones and filters and sequestered. The recovery of carbon or iron is not considered in this study. Their recovery will require an additional separation process. The rich-hydrogen gas product is fed to the PSA to remove any remaining oxides of carbon, water vapor, methane, and traces of hydrocarbons. 90% of the hydrogen is assumed to be recovered at a PSA operating pressure of 2,010 kPa. The recovered hydrogen gas is sent to the ammonia synthesis unit. Flue gasses leaving the furnace radiant zones of the reactors preheat boiler feed water to generate super-heated steam in a waste heat boiler. The super-heated steam drives some compressors to reduce electrical loads.

Air separation unit

A multi-stage compressor with intercooling is used to compress air at a pressure of 6.35 bar. A mechanical filter cleans the compressed air placed at the inlet of the compressors. The cooled air is split in two. One of the split streams is re-compressed in a multi-stage compressor, cooled, liquified using product streams in a heat exchanger, and expanded. It then enters a high-pressure column (HPC), where nitrogen is removed as

a top product. A side stream is withdrawn from the HPC. The stream is partially liquefied using product streams in a sub-cooler. It is then depressurized before entering a separator where its bottom stream enters the LPC and the top as waste. HPC operates at a pressure of 6.0 bar. The other split stream is partially liquefied using the product streams in a sub-cooler. The partially liquified stream is also split into two. One of the split streams enters the HPC, while the other enters the low-pressure column (LPC). LPC operates at 1.2 bar. HPC bottom product (rich in oxygen) enters the LPC after being cooled by the product streams in a sub-cooler and then depressurized. Nitrogen and oxygen leave LPC as top and bottom products, respectively. A side product from LPC leaves as waste.

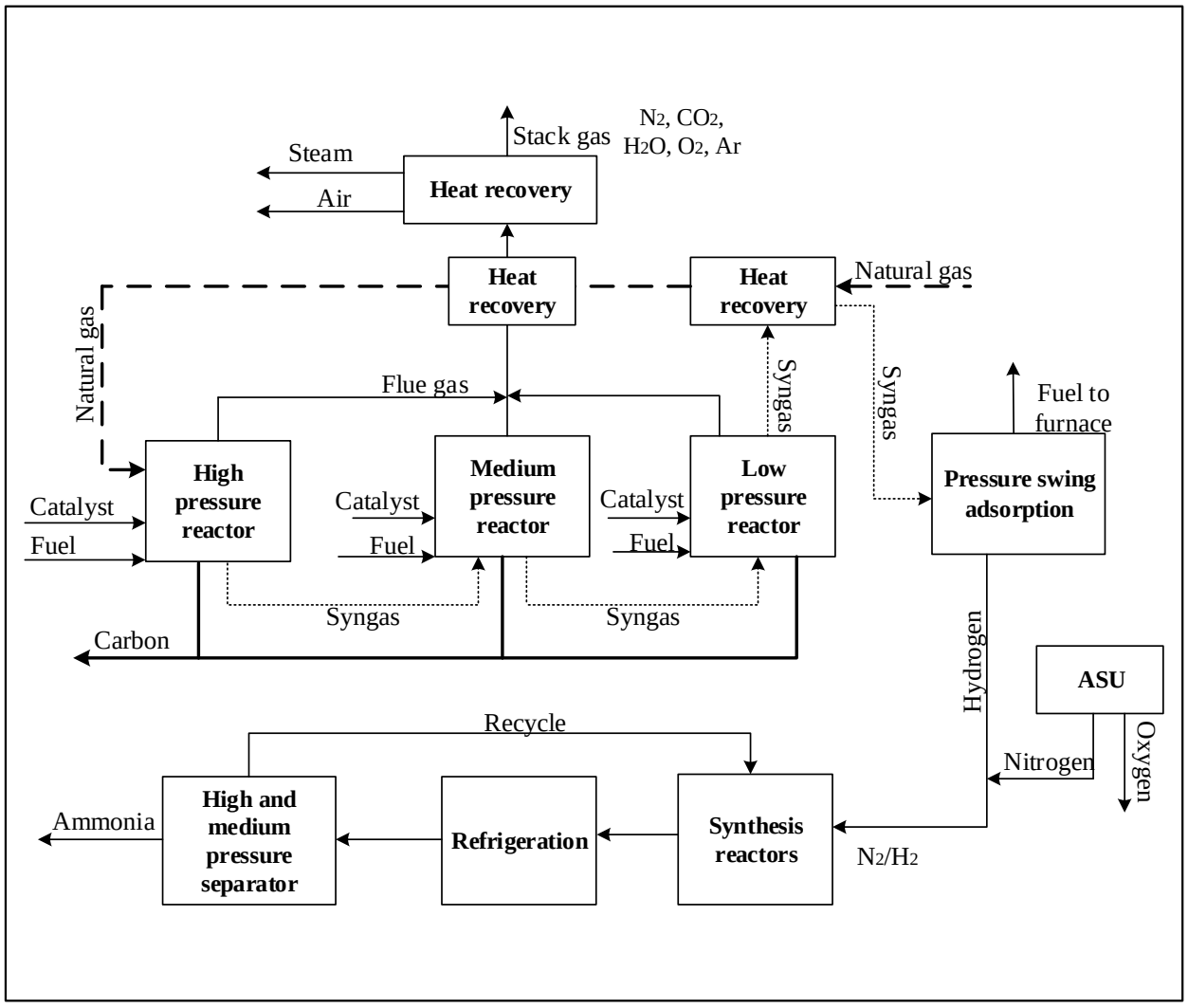

Fig. 2: Schematic diagram of ammonia production through the TDM pathway

2.2 Process simulation

Using Aspen HYSYS simulation software, a detailed process model was developed for each process to obtain the material and energy balances. The resulting energy and material balance were used to determine the equipment size and process economics. The Peng-Robinson equation and ASME steam table correlations for thermodynamic properties are used for the predictions of the components in the processes. Following Fig. *1* and Fig. *2*, the chemical reactions occurring in each reactor were modeled using the Equilibrium Reactors in Aspen HYSYS. Details of the chemical reaction and their kinetics are provided in Appendix A1.

2.3 Energy consumption and GHG emissions evaluation

Fig. 3 presents the system boundary of the ammonia production processes. The performance of each process was determined by evaluating energy use and GHG emissions. The energy inputs for electrical devices are obtained from the simulation models using the appropriate efficiencies.

GHG emission was evaluated using the LCA framework according to the International Organization for Standardization (ISO) recommendations [32, 33]. One tonne of the produced ammonia is considered the functional unit to which the GHG footprint as kilograms of CO_2-equivalent gas emitted ($kgCO_2e$) is normalized. Table 1 presents the emission factors for natural gas and electricity. For natural gas, both combustion and upstream emissions were considered. The electricity emission factor for the base case scenario was based on the Alberta grid emission intensity for 2020. A combined heat and power (CHP) plant provides lower emission intensity than the Alberta electricity grid. For this reason, the impact of a CHP plant was considered on the life cycle GHG emissions.

For the base case scenario, we assume a global warming potential of 100 years (GWP-100) time horizon, which is recommended by IPCC. In recent times, some scientists have promoted the use of a global warming potential of 20 years (GWP-20) time horizon. The latest IPCC AR6, using methane as an example, it was discussed the use of a range of emission metrics, including GWP-20 and GWP-100, and how they perform [34]. IPPC AR6 provides an insight into how cumulative CO_2 equivalent emissions for methane vary under

different emission metric choices and how the global surface air temperature (GSAT) compares with the actual temperature response. They argue that a drop in methane emissions could cause global warming to decline. The trend in global surface air temperature (GSAT) estimated with cumulative CO_2 equivalent emissions computed with GWP-20 matches the warming trend for a few decades but quickly overestimates the response. Cumulative emissions using GWP-100 perform well when emissions are increasing, but not when they are stable or decreasing. For these reasons, we also considered the impact of global warming using the GWP-20-time horizon. Table *2* presents the GWP-100 and GWP-20 for the greenhouse gases considered in this study.

It is important to mention that for emissions associated with natural gas, we considered both combustion and upstream emissions. The 5-year average of Alberta natural gas recovery, processing, transmission, and distribution emissions is 8.88 kg-CO_2eq/ GJ of natural gas produced [35, 36].

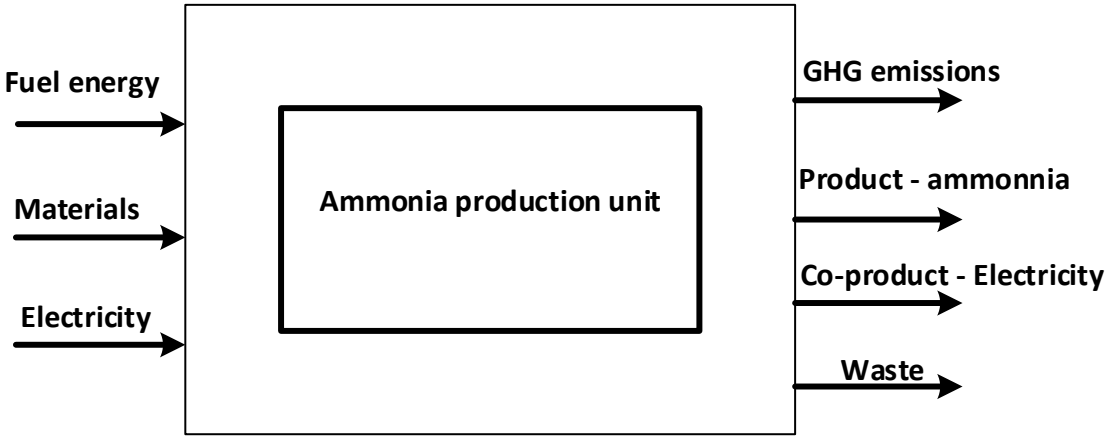

Fig. 3: System boundary for the ammonia production pathways

2.4 Economic analysis

The production cost of ammonia was calculated using discounted cash flow (DCF) analysis. The basic assumptions for the DCF analysis are shown in Table 3. Capital investment and cost of manufacturing (COM) were evaluated. The costs of pumps, compressors, expanders, heat exchangers, fans, and coolers

were estimated using the Aspen plus economizer. Using a conservative scale factor of 0.6, the cost of SMR reactors, ammonia synthesis reactors, TDM reactors, and pressure swing absorption were calculated from previous analysis by Salkuyeh et al. [37], Bartels [38], Spath and Lane [39], and Larson et al. [40] and Kreutz et al. [41], respectively. Table 4 summarizes the general assumptions for capital cost estimation. The manufacturing cost includes direct manufacturing cost, fixed manufacturing cost, and general expenses. Details of each manufacturing are provided by Turton [42]. The cost of manufacturing (COM) is evaluated using Equation (1) [42].

$$COM = 0.18\,FCI + 2.73(operating\ labor) + 1.23(Utilities + Cost\ of\ raw\ material) \quad (1)$$

where FCI is fixed capital investment.

Table 1: Model assumptions for the analysis

Parameters	Value
Reboiler efficiency, %	90.0
Compressor efficiency, %	87.0
Natural gas expander efficiency, %	75.0
Turbine efficiency, %	87.0
Pump efficiency, %	87.0
Fan efficiency, %	65.0
Pressure difference for pumping cooling water, kPa [42]	266.0
Upstream emissions of natural gas, kg CO_2eq/GJ [35, 36, 43]	8.9
Emission factor of natural gas, kgCO_2eq/GJ [43]	55.8
Emission factor of the biomass-fired power plant, kgCO_2e/MWh [44]	80.0
Emission factor of Alberta grid electricity (2020 mix), kg CO_2eq/MWh[45]	544.4
Emission factor of electricity from CHP, kg CO_2eq/MWh [46]	367.0

Table 2: IPCC Sixth Assessment Report Global Warming Potentials (AR6 2021) [34]

Greenhouse gas	100-year period	20-year period
CO_2	1	1
CH_4 fossil origin	29.8	82.5
CH_4 non-fossil origin	27.2	80.5
N_2O	273	273

Table 3: Assumptions for the economic model

Parameter	Values
Base year	2020
Capacity utilization	90%
Internal rate of return (IRR)	10%
Plant lifetime	25 years
Decommissioning cost	2.3% FCI
Construction payment years	3

264

265 Table 4: Assumptions for the estimation of capital cost and COM

Economic data	Value	Reference
Capital investment		[47]
Total Purchase Equipment Cost (TPEC)	100% TPEC	
Total Installed Cost (TIC)	203% TPEC	
Indirect Cost (IC)	89% TPEC	
Total Indirect Cost (TDIC)	TIC + IC	
Contingency	20% TDIC	
Fixed Capital Investment (FCI)	TDIC + Contingency	
Location factor (LF)	10% FCI	
Total Capital Cost	FCI + LF	
Operating cost		
Process water	0.067$/tonne	[42]
Natural gas	1.96$/GJ	
Electricity	0.06$/kWh	[42]
Catalyst (primary reformer)	10$/kg	[13]
Catalyst (secondary reformer)	15$/kg	[13, 48]
Catalyst (Methanation)	17.7 $/kg	[13]
Catalyst (iron ore)	169$/tonne	[49]
MEA	1250 $/tonne	[50]
Oxygen price	40 $/tonne	[51]
Ammonia price	593.94$/t NH_3	[52]

266

267

3. Results

This section provides insight into using SMR and TDM pathways for ammonia production. Each pathway produces 2,215 tonnes of ammonia per day. The pathways are assessed based on process parameters (operating variables and material use), energy consumption, and greenhouse gas emissions. Fig. 4 and Fig. 4 present model results of the SMR and TDM pathways, respectively. Model accuracy relies on the appropriate reaction kinetics, plant configuration, and operating conditions. These factors were considered in the model development for an accurate representation of each process. For completeness, the compared our model results were compared with process data in the literature. The results show good agreement with typical plant data.

3.1 SMR pathway

3.1.1 Model analysis

Important process variables are steam-to-carbon ratio, methane slip, nitrogen-to-hydrogen ratio, and oxidant slip. Ensuring tight control of these variables results in optimal fuel use, economic benefits, and improved efficiency. For the feed stream to the primary reformer, a steam-to-carbon ratio of 3.0 was maintained to control methane slippage at the reformer outlet, maximize yield, and reduce steam production costs. As earlier mentioned, a lower steam-to-carbon ratio leads to increase in heating demand. The steam-to-carbon ratio may vary depending on the process configuration. For example, the Kellogg ammonia technology, KRES, operates with a steam-to-carbon ratio in the range of 3.0-4.0 [26]. In the KRES configuration, a higher steam-to-carbon ratio is implemented by feeding some of the feed streams directly into the secondary reformer. Thus, increasing the volume of methane in the secondary reformer above a typical plant level. In the configuration studied, the primary reformer inlet and outlet stream temperatures were regulated to maintain a methane volume of 10.2% (13.6% dry basis), in line with what a typical industrial plant operation maintains of 10.0% (13.0% dry basis) [26, 53]. This volume of methane contributes to the supply of heat needed in the secondary reformer. The reminder exits as an effluent. The reformer's effluent heat is integrated using heat exchangers to generate the steam needed within the plant.

293 The air supplied to the secondary reformer provides the oxygen to burn a certain quantity of the reformed
294 gas and natural gas. Compared to the standard combustion process, the oxidant (oxygen) is less than the
295 fuel. Thus, leaving no traces of oxygen in the exiting stream and unreformed methane (slippage) reduced
296 to about 0.1%. The air supplied also gave a 3:1 ratio of hydrogen-to-nitrogen needed for ammonia synthesis.
297 Using the WGS reactors, the hydrogen to nitrogen ratio increases to 3.0, which is sufficient to meet the
298 hydrogen demand for ammonia production. Thus, reducing the carbon monoxide content in high and low
299 temperature WGS reactors to 2.4% and 0.2%, respectively. These values are in close agreement with that
300 reported by McVickar et al. [53]. Furthermore, the low temperature WGS's (LT-WGS) gas composition
301 from these simulation results fairly agrees with typical plant data [53]. The compositions of the converted
302 gas by the LT-WGS presented by McVickar et al. are (percent by volume, dry basis): CO_2 17.6; CO 0.2;
303 H_2 61.5; N_2 20.5; and CH_4 0.2, and in this work CO_2 27.8; CO 0.3; H_2 51.1; N_2 20.1; and CH_4 0.1. The
304 percentage mole composition of the gases leaving the LT-WGS is presented in

Table 5. The MEA scrubber and methanation are the final purification steps, where carbon dioxide and carbon monoxide are removed and converted to methane, respectively. The oxides of carbon in the gas flow to the ammonia synthesis unit are less than 10 ppm. In the ammonia synthesis unit, the percentage conversion of reactants to ammonia is 28%. The molar flow ratio of the recycled gas to the fresh syngas is 3.0, and the purity of ammonia produced is 99.2%. The simulation results for gas composition from the WGS reactors, methanation, amine scrubbers, and ammonia synthesis agree with typical plant data (see Table 5)

313

314 Table 5: Comparing the results obtained in this study with gas components (mol%, dry basis) leaving various units of the ammonia plant

	Primary reformer		Secondary reformer		HT-WGS		LT-WGS		Methanation		Ammonia tank	
Reference	A	B	A	B	A	B	A	B	A	B	A	B
CH_4	14.13	8.67	0.6	0.2	0.53	0.1	-	0.10	1.16	0.31	0.12	0.24
CO_2	10.11	9.44	7.38	6.4	18.14	15.73	-	18.10	-	-	-	-
CO	9.91	11.51	13.53	14.65	0.33	3.23	-	0.29	-	-	-	-
H_2	65.52	69.82	54.57	55.74	59.85	60.15	-	61.31	73.54	74.68	0.03	0.14
N_2	0.33	0.32	23.64	22.93	20.9	20.65	-	20.01	24.93	24.67	0.02	0.02
NH_3	-	-	-	-	-	-	-	-	-	-	99.82	99.18
Others	0.00	0.26	0.28	0.08	0.25	0.15	-	0.19	0.37	0.34	0.01	0.42

A: KRES [26] B: This study

315

3.1.2 Energy consumption

Table 6 presents the energy consumption pattern of the SMR pathway. The total natural gas consumed by the process is 31.9 GJ/t NH_3. This value is in close agreement with studies by Appl [25, 26] (28-29.3 GJ/t NH_3), Smith et al. [54] (27.4-31.8 GJ/t NH_3), and Natural Resources Canada [55] (33.8-38.6 GJ/t NH_3) for the Haber-Bosch process plant. The energy input to the process includes natural gas fuel, electricity, and heat gained from the process through exothermic reactions. The total energy supplied to the pathway was estimated to be 23.2 GJ/t NH_3. Electrical devices such as pumps and compressors consume 18.4% (3.8 GJ/t NH_3). The fuel energy supplied for process heating was estimated to be 15.7 GJ/t NH_3. Part of the natural gas feedstock contributes to the process heating in the secondary reformer. For this reason, it was included in the process efficiency calculation. The total energy gained because of exothermic reactions occurring in methanation reactor, WGS reactors, and synthesis reactor is 3.9 GJ/t NH_3. Using these heat of reactions raises the process energy efficiency to 68.7%. This efficiency is comparable to 64.6% reported by Appl [56]. About 74.9% of the energy loss in the process occurs in the WGS and methanation units. Most of these losses are low-grade heat cooled off. The primary reformer accounts for 83.4% of the fuel energy supplied, making it the most energy-intensive unit. Its efficiency reaches 90% because it is well-integrated to use heat efficiently. The fuel gas leaving the reformer generates 1.85 GJ/t NH_3 to preheat natural gas and air and produce steam. The combustion of natural gas in the secondary reformer generates 6.0 GJ/t NH_3. The endothermic reactions occurring in the secondary reformer account for 59.1% (3.6 GJ/t NH_3) of the energy produced through natural gas combustion. Part of the remainder, released as effluent, generates steam needed in the primary reformer and MEA regenerator. The use of this heat, about 9.7 GJ/t NH_3, for producing steam is a major contribution to the process efficiency.

Table 6: Energy analysis of the SMR pathway (GJ/t NH_3)

Parameter	Energy inputs	Losses
Primary reformer fuel	9.71	0.68
Secondary reformer	6.03	0.00
Ammonia synthesis	3.09	1.94
High WGS	0.29	0.00
Low WGS	0.27	2.70
Methanation	0.02	0.55
MEA unit	0.00	1.34
Electricity	3.74	0.48
Total	23.55	7.70

341

342

343 3.1.3 GHG emissions

344 The life cycle GHG emissions are 2.51 $tCO_2e/t\ NH_3$. The largest share of the GHG emissions is onsite, and
345 it accounted for 66.2%. The onsite GHG emissions are from two sources, flue gases from the reformer and
346 the separated CO_2 gases leaving through the regenerator. The CO_2 emissions leaving through the (or process
347 emissions) regenerator represent 67.4% of the onsite CO_2 emissions, which show the potential to
348 significantly lower overall emissions if captured and sequestered. The emission from electricity is also
349 significant, and it accounts for 22.5% of the life cycle GHG emissions. The upstream of natural gas is a
350 small part (11.3%). Upstream emission is due to the recovery, processing, and transportation of natural gas
351 to the plant site.

352 3.1.4 Economic assessment

353 The production cost of ammonia from the SMR pathway was estimated to be \$500/t NH_3. The capital cost
354 and manufacturing cost (COM) were estimated to be \$807 M and \$340 M/year, respectively. For capital

investment, the major cost components are from the reformers and WGS units. These components (reactors, compressors, pumps, heat exchangers, and coolers) account for 54.6% of the capital investment. The ammonia synthesis unit (synloop and storage) and purification unit (amine scrubbers and regenerator) account for 33.2% and 19.2%, respectively. For COM, the direct cost, which includes raw material, utilities, labor, and so on, plays a significant role. They account for 58.8% of COM. These results are comparable to the production cost of ammonia reported by Appl [26] and Rutkowski [38, 57] of \$495/t NH_3 and \$521/t NH_3, respectively, in 2007. If their values are adjusted for inflation to the year 2020, the cost of ammonia will be \$505/t NH_3 for Appl and \$531/t NH_3 for Rutkowski. The differences in results might be due to input assumptions and operating cost like natural gas price. Furthermore, according to Bartels [38], the cost of ammonia from a coal-based plant is usually low, from 147-432 \$/t, while a natural gas-based plant ranges 395-688 \$/t. When carbon capture and storage (CCS) is installed into the two sources of CO_2 emissions, the production cost of ammonia increased by 28.6% (\$143/t NH_3). Sequestering only the separated CO_2 gases leaving the amine regenerator leads to an increase in ammonia cost by 11.1% (\$65/t NH_3). For a capacity of 2,004 tonnes of ammonia per day, a percentage increase of 7.7% (\$40/t NH_3) for sequestering CO_2 gases was estimated from Rutkowski [38, 57]. This value is close to the value reported in this study. Lastly, a government implemented carbon pricing benchmark of \$99/t CO_2 is equivalent to integrating a CCS into an ammonia plant. Thus, economically, the CCS is worth implementing with a carbon price above this value.

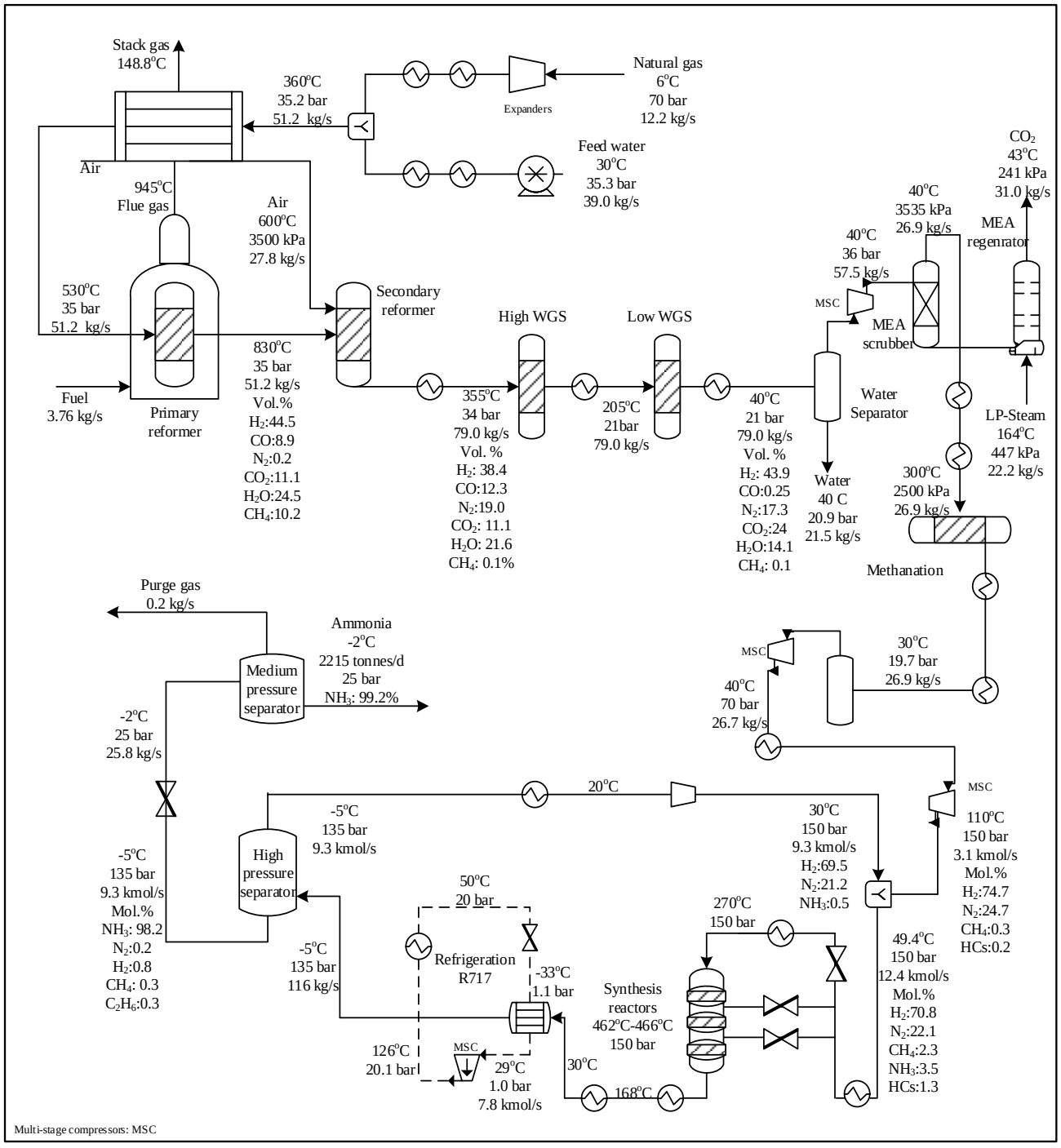

Fig. 4: Simulation results of the SMR pathway for ammonia production

3.2 TDM pathway

3.2.1 Model analysis

Fig. 5 presents a material balance of the TDM pathway. The reactor temperature and pressure play a key role in natural gas conversion. A what-if analysis was performed to determine a suitable operating condition of the TDM reactors (HPR, MPR, and LPR). The reactors' pressure and temperature were varied between 3500 - 110 kPa and 900^{o}C-850^{o}C, respectively. Accordingly, the optimum pressure for HPR, MPR, and LPR is 2,100 kPa, 450 kPa, and 110 kPa, respectively. With the reactor temperature at 850^{o}C, overall natural gas conversion at these pressures is 94.7%. The percentage conversion of natural gas in HPR, MPR, and LPR is 54.0%, 59.1%, and 71.8%, respectively. The rate of conversion increased in MPR and LPR because pressure drop across the reactors favors hydrogen yield. Low pressure favors the shift of reaction equilibrium towards hydrogen product. The product stream contains 95.3% hydrogen by mole filtering off the solid carbon. Keipi et al. [21] reported a methane conversion of 40% and hydrogen concentration of 57.1 wt.% for a single fluidized bed reactor. In an experimental study by Suelves et al. [58], they reported hydrogen concentration of 80% (mol.) at 700^{o}C using a Ni-based catalyst in a single reactor. Methane conversion was 67%. These findings compared reasonably with 61.1 wt% hydrogen concentration in the HPR (present study). Steinberg also reported 90% (mol.) for thermal decomposition of natural gas in a molten metal reactor [59]. The thermal conversion of natural gas to hydrogen depends on many factors, such as the number of reactors, operating conditions, and the type of catalyst used. The variation in these results is due to these factors.

The unreacted components in the gas stream leaving the reactor are separated and used as fuel. These components make about 44.0% of the fuel used to provide heat to the reactors. Hydrogen volume flow in the unconverted stream is 51.7%. This value reduces to 28.5% when combined with natural gas fuel supplied to heat the reactors. The carbon produced per tonne of ammonia is 0.53 and with a purity of 94%. The purity was determined based on the amount of the iron oxide catalyst in carbon. Deactivated catalysts are not reused or regenerated but replaced with new ones. The carbon product can be an additional marketable product. However, the current global demand for carbon is low [60]. The ASU produces

nitrogen to meet a nitrogen-to-hydrogen ratio of 3.0. The by-product, oxygen, is valuable, and it is likely to find a market that can accommodate production. The purity of nitrogen and oxygen product in the ASU is 98.0%. The ASU waste stream is a less valuable product, and it was used as an oxidant for fuel combustion. In the ammonia synthesis reactors, the percentage conversion of reactants to ammonia is 28%. The molar flow ratio of the recycled gas to the fresh syngas is 3.0, and the purity of ammonia produced is 99.5%.

3.2.2 Energy consumption

Table 7 presents the specific energy of the process units in the production of ammonia using the TDM technology. The total natural gas used as feedstock and fuel is 49.3 GJ/t NH_3. A reduction in this value can only be realized by lowering the fuel requirement because the actual feedstock needed for ammonia production is by stoichiometry. One way to reduce the natural gas demand is by lowering the operating temperature of the reactors. However, reducing the reactor temperature will require a more active catalyst that would increase the reaction rate by lowering the reaction activation energy. Many studies have shown that methane decomposition can occur at a low temperature between 550-650^{o}C using Ni catalyst [61], Ni/SiO_2 catalyst [62], or $Fe–Mo/Al_2O_3$ catalyst [63]. A more radical step is to use carbon products as fuel, but it would increase carbon emissions. Nonetheless, the total fuel required for heating the reactors is 9.12 GJ/t NH_3 (a mixture of natural gas and recycled hydrogen and heavy hydrocarbons). Electricity for pumps, fans, and compressors makes 4.10 GJ/t NH_3. The total energy loss in the process is 6.15 GJ/t NH_3. Most of the losses occurred in the synthesis unit and decarbonization unit. In the synthesis unit, the reaction heat of ammonia synthesis is 6.13 GJ/t NH_3. About 54.2% preheats the feed streams to the synthesis reactor. The remaining 2.81 GJ/t NH_3, is wasted through cooling. This heat can provide low-pressure steam, but it is of no use in the current design of the TDM pathway. The decarbonization unit is another important part of the process and the most energy intensive unit. Its reactors consume 51.3% of the fuel (natural gas) supplied to provide heat for thermal decomposition of natural gas. The remaining part of the energy is embedded in the flue gas, which leaves the reactor at 960^{o}C. To avoid huge losses and improve energy efficiency, the flue gas is used to preheat combustion air, natural gas, and generates steam to drive a turbine. The energy gained by these streams lowers the heating and electrical loads by 0.57 and 0.46 GJ/t NH_3, respectively. By

adopting this approach, the efficiency of the reactor's furnace reaches 77.8% from 51.3%. The resulting flue gas leaves the furnace stack with an energy loss of 2.02 GJ/t NH_3. The calculated initial efficiency value is comparable to 58% reported for the thermal decomposition of methane [59]. Overall, the energy efficiency of the TDM pathway is 68.2%.

Table 7: Energy analysis of the TDM pathway (GJ/t NH_3)

Parameter	Energy inputs	Losses
Natural gas fuel to reactors	6.56	2.82
H_2 in fuel mixture to reactors	2.56	-
Ammonia synthesis	6.13	2.81
Electricity	4.07	0.53
Total	19.32	6.15

3.2.3 GHG emissions

The life cycle GHG emissions are 1.42 $tCO_2e/t\ NH_3$. GHG emission from electricity takes the largest share, 42.8% of the overall emissions. These emissions are due to the compression of gases, especially in the ammonia synthesis and ASU units. Onsite (GHG emissions because of fuel combustion) and natural gas upstream emissions account for 30.8% and 25.8%, respectively. The inefficiencies associated with the recovery of heat from the furnace stack impact onsite emissions. Upgrading the furnace efficiency from 77.8% to a typical value of 90% could lower onsite emissions by 5.0%. TDM produces carbon to avoid producing CO_2 emissions in its reactors, thus, reduce the overall emissions associated with the production of ammonia. The CO_2 emissions potential of the produced carbon (9,091 tonnes) is 15.0 $tCO_2e/t\ NH_3$. Some studies suggest using the carbon product as fuel or gasification agent [21, 22]. However, using carbon as fuel in the TDM reactors will increase onsite CO_2 emission by 0.37 $tCO_2e/t\ NH_3$. The increase in

combustion emissions is twice the base case value. With a carbon lower heating value of 32.8 MJ/kg, we estimated the amount of carbon required for combustion to be 1,624 tonnes per day.

3.2.4 Economic assessment

The production cost of ammonia from the TDM pathway was estimated to be \$569/t NH_3 without considering product oxygen. Integrating CCS leads to an increase in the production cost of ammonia by 13.4% (\$76/tNH_3). The capital investment and COM of the process (without CCS) is \$946 M and 382 \$M/year, respectively. For capital investment, the major cost components are from the hydrogen production units. The components in these units (reactors, compressors, pumps, heat exchangers, and coolers) account for 48.1% of the capital investment. The ammonia synthesis unit, the air separation unit, purification unit account for 25.0%, 15.7%, and 11.2%, respectively. For the operating cost, the consumption of natural gas, electricity, and maintenance cost play a significant role. Other cost parameters such as cooling water, labor, etc., have less influence. A breakdown of the TDM and SMR costs is presented in appendix A2.

Product oxygen is valuable. Its market value represents additional revenue to the TDM pathway, thus lowering the cost of ammonia products. So, we analyzed the effect of product oxygen as well. Based on an oxygen selling price of \$40/t O_2, the cost of ammonia is \$560/t NH_3, a reduction in the base case by 1.6%. The sale of an oxygen product does not significantly reduce the cost of ammonia. Lastly, a government implemented carbon pricing benchmark of \$57/t CO_2 is equivalent to integrating a CCS into an TDM ammonia plant. So, economically, the CCS is worth implementing with a carbon price above this value. It is worth mentioning that the economic impact of carbon and the regeneration of the iron catalyst is not considered in this study. The mixture (carbon and iron) requires a recovery process. Regenerating the iron catalyst through combustion is a popular approach, however, these would release CO_2 emissions. Capturing these CO_2 emissions would add to the overall cost of ammonia. It is therefore unclear whether these byproducts will add economic value to the TDM process. It would be interesting to consider the addition of these processes in future work.

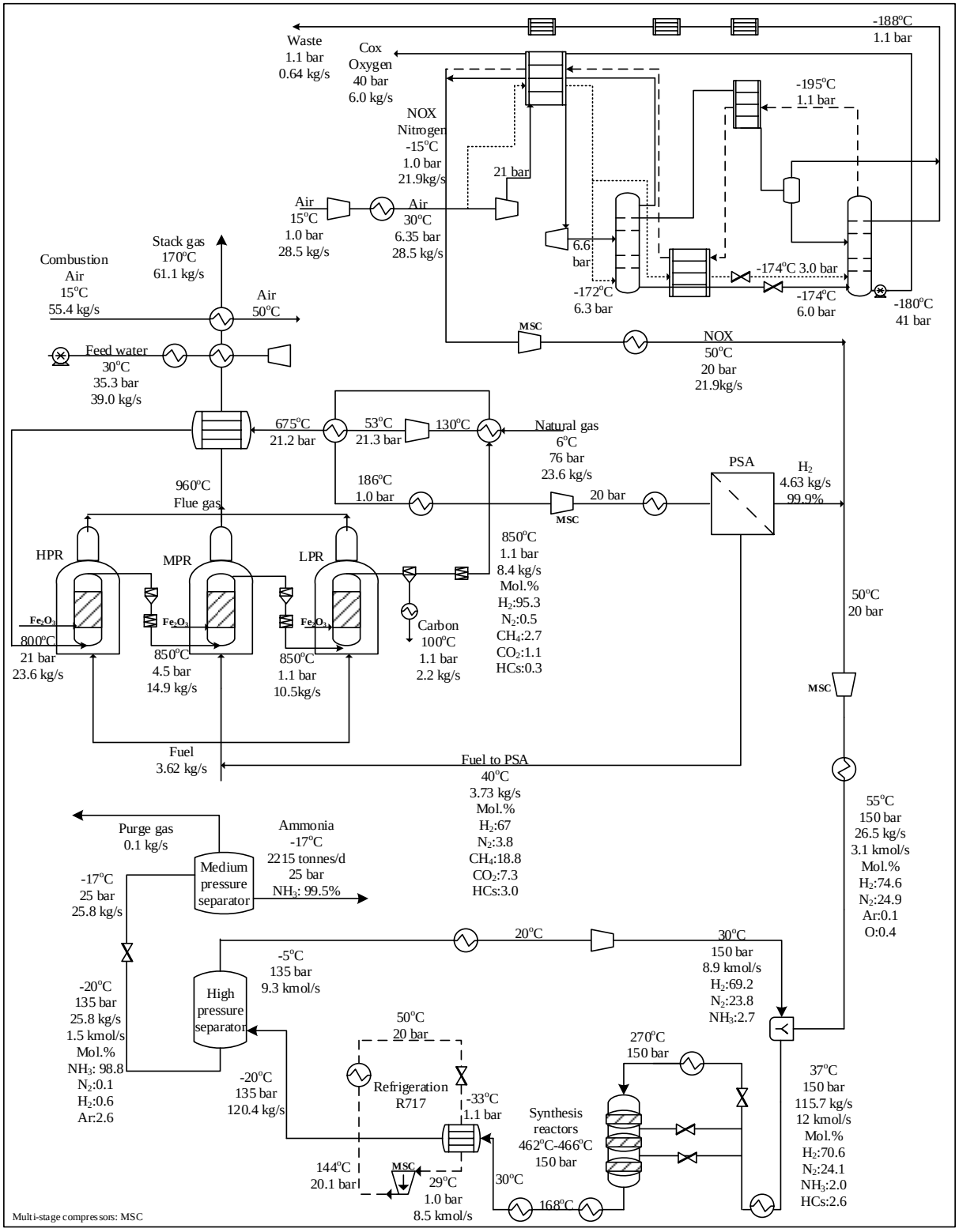

Fig. 5: Simulation results of the TDM pathway for ammonia production

3.3 Sensitivity and uncertainty analyses

3.3.1 Economic analysis

Using point estimates to examine the output of a model can sometimes mislead when the uncertainties in the inputs have significant effects. To understand how the uncertainties in the assumptions used in this study affect the economic output of both technologies, sensitivity and uncertainty analyses were conducted. The relative uncertainty used for all the economic inputs was 30%. This value is commonly used to analyze the variability in economic inputs. The Morris global sensitivity method was used to determine inputs that have a strong impact on the cost of ammonia in each case. Fig. *6* (a and b) shows how the uncertainties in the input assumptions impact the production cost of ammonia. Sensitive inputs have a high Morris mean, moderately sensitive have a relatively low Morris mean, while inputs at zero (or close to zero) are not sensitive. In both cases, SMR and TDM, the capital cost is the most sensitive input, contributing 76.1% and 72.6% to the output uncertainty, respectively. IRR, contingency, natural gas, and electricity are moderately sensitive, while the remaining inputs are not sensitive (many of which are not shown in the figures for brevity). Only sensitive inputs are considered for uncertainty analysis. Fig. *7* shows the box plot representation of the uncertainty results for each case. The plot depicts how the uncertainty in inputs affects the cost of ammonia in the TDM and SMR technologies. The overlap (in Fig. *7*) in the cost of ammonia makes it difficult to determine which case is more economically favorable. Further analysis is required to determine the most suitable technology. Henriksson et al. [64] recommended a four-step method for comparison, which are quantifying and characterizing input parameters (step 1), quantifying output uncertainties using propagation methods like Monte Carlo (step 2), statistical testing (step 3), and communicating results (step 4). This method allows for an accurate comparison between technologies because data considered for analysis is dependent, so each technology uses the same sampled inputs. Using Henriksson et al.'s four-step method, we ran a Monte Carlo simulation with sampled inputs. Here, we evaluated the differences in each Monte Carlo simulation by subtracting the economic output of both technologies to determine the most preferable. Fig. 8 shows the differences in the economic output of both technologies. Each point on the curve represents the differences between the probable outcomes of the two

technologies. Because we subtracted the cost of SMR-based ammonia from TDM ($/tNH$_{3\ TDM}$ - $/tNH$_{3\ SMR}$ = Δ $/tNH$_3$), a negative output favors the TDM while a positive favors SMR. Fig. *8* shows that it is more likely that the ammonia produced from the SMR technology will be economically preferable to the TDM. The likelihood of TDM being a preferable choice is less than 20%. The TDM achieves this favorability at its lowest capital cost and the highest capital cost of SMR. The curve is driven by the capital cost of TDM and SMR. The capital cost of SMR and TDM account for 63.8% and 28.9% of the distribution, respectively.

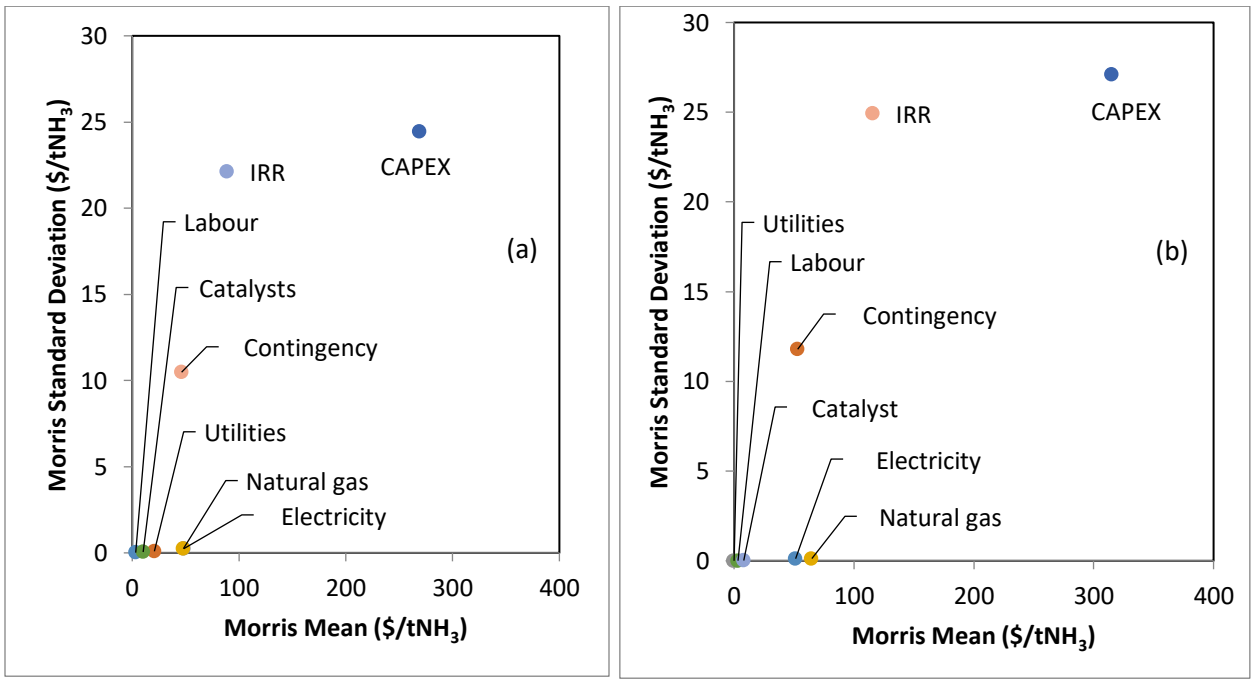

Fig. 6: Morris's sensitivity result for the SMR (a) and TDM (b)

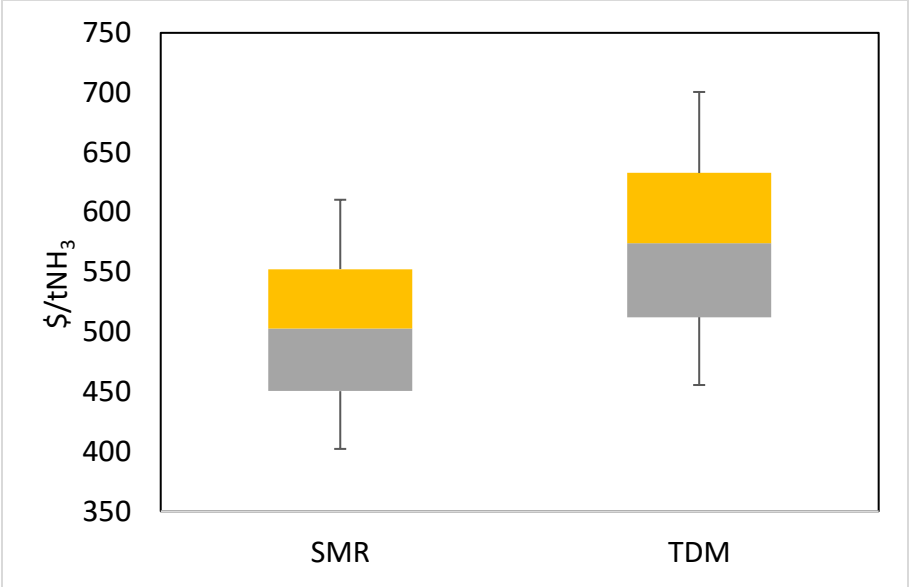

513

514 Fig. 7: Comparison the cost of ammonia production from SMR and TDM, legend: top error bar: P95; top
515 box side: P75; middle line: mean; bottom box side: P25; bottom error bar: P5

516

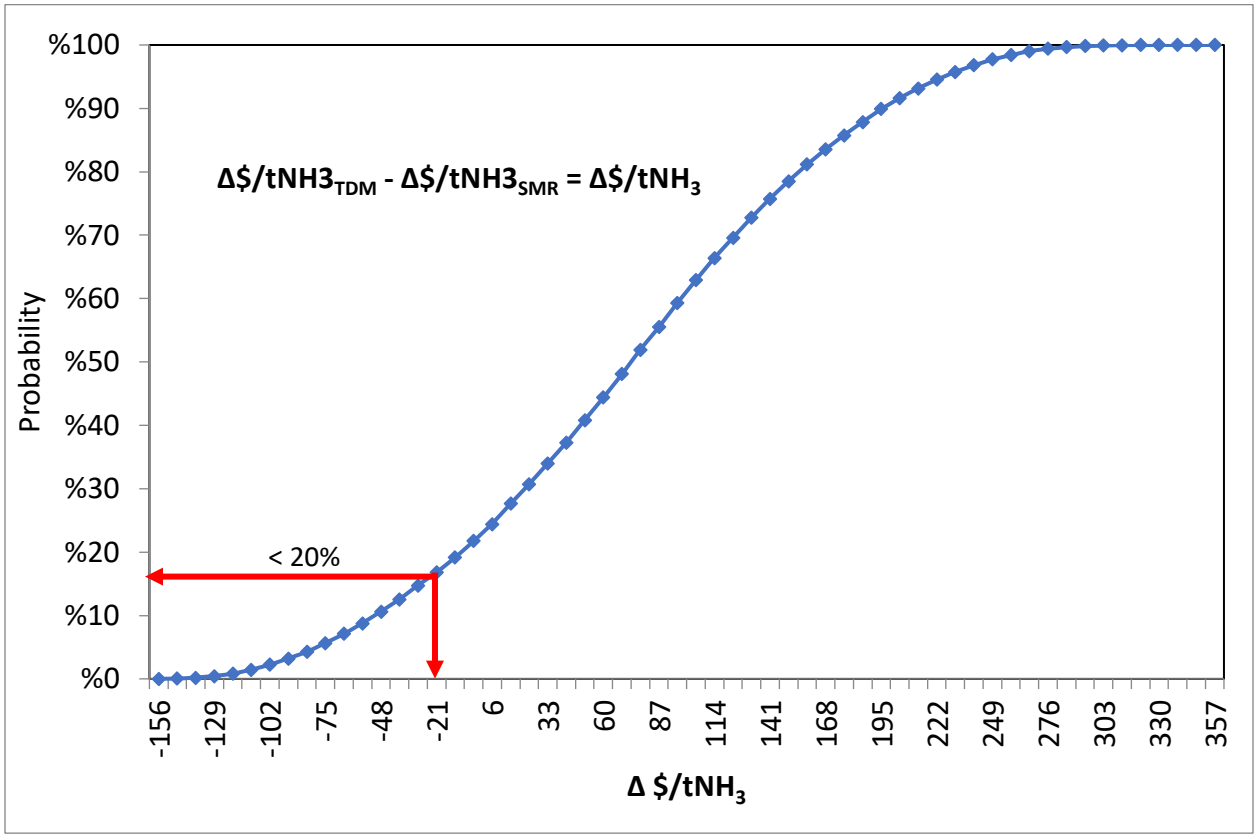

517

518 Fig. 8: Differences in the cost of ammonia produced from TDM ($/tNH$_3$) and SMR ($/tNH$_3$), Δ $/tNH$_3$

519

3.3.2 GHG emissions

Fig. *9* compares the uncertainties in both pathways (without CCS). Clearly, the figure shows that irrespective of the uncertainty in the inputs, the GHG emission of the TDM is lower than the SMR. The relative GHG emissions uncertainties were estimated to be 34.5% (±0.49) and 14.5% (±0.36) for the TDM and SMR, respectively. In the TDM and SMR pathways, the output GHG emissions are mostly driven by the uncertainty in upstream natural gas emissions, contributing 79.7% and 60.5%, respectively. Upstream natural gas emissions can vary widely from site to site. As earlier mentioned in section 2.4, the base case value (8.88 $kgCO_2e/GJ$) was a five-year average reported by Canada Energy regulator [35] and Environment and Climate Change Canada [36]. MacKay et al. reported that Canada's upstream natural gas emissions value may be underestimated because most measurement studies in Canada comprise relatively region-specific sample populations, which may not be extensible to regions with varying extractive techniques, geology, and geochemical properties [65]. To account for these variations, we used an uncertainty value of 100% (±8.88 $kgCO_2e/GJ$). This value (17.76 $kgCO_2e/GJ$) is close to the upper bound reported in some studies [65, 66]. Their (TDM and SMR) corresponding electricity emission contributes 16.8% and 25.7% to the output while natural gas combustion contributes 3.5% and 13.8%, respectively. The relative uncertainty used for electricity emissions and natural gas combustion is 33% and 25% [67], respectively.

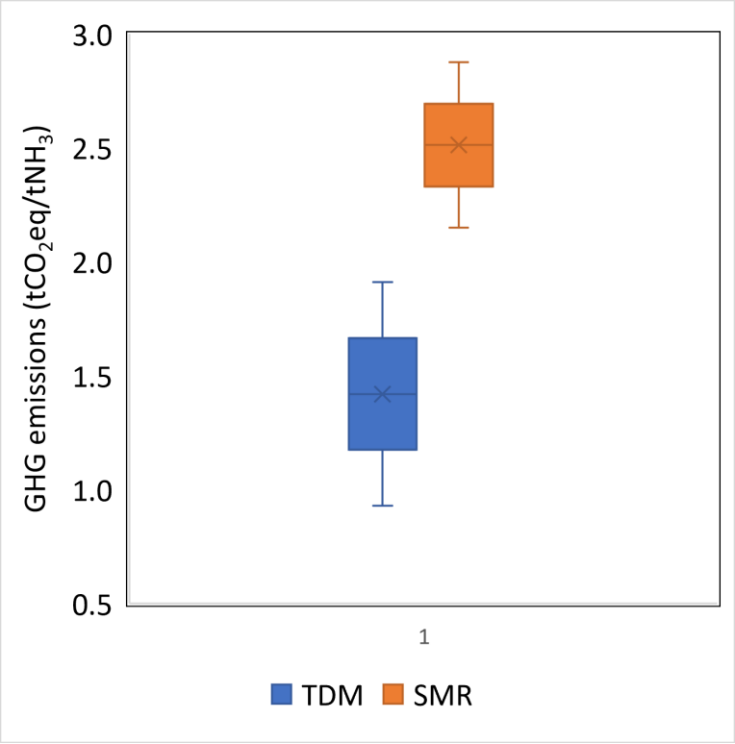

538

539 Fig. 9: Comparing the GHG emission uncertainty of the TDM and SMR technologies, legend: top error bar:
540 P95; top box side: P75; middle line: mean; bottom box side: P25; bottom error bar: P5

541

542 3.4 The effect of using the 100-year or 20-year time-horizon global warming potential

543 GWP-100 and GWP-20 estimates were used to describe the impact of the different greenhouse gases
544 released into the air by the processes (TDM and SMR). Most important GHGs for this study are CO_2, CH_4,
545 and N_2O and their environmental effects in 100-year and 20-year time horizons. Fig. 10 (a and b) compares
546 the GWP-100 and GWP-20. For both processes, the GWP-20 has a higher global warming effect, mainly
547 because of the natural gas (methane) upstream emissions, which account for about 98% of the total increase
548 in each case. The application of GWP-20 to TDM and SMR increases their global warming potential by
549 7.0% and 2.6%, respectively, when compared with GWP-100. The upstream emissions associated with
550 natural gas (methane) use dominate the overall increase in the global warming potential. However, like the
551 GWP-100, the GWP-20 estimates also suggest that TDM is a favorable technological choice. TDM has a

lower global warming potential than the SMR even with its relatively high natural gas consumption. These results also show that our discussion on uncertainty analysis using GWP-100 holds for GWP-20.

Global warming impact can also occur through hydrogen leakage, venting, and purging from these ammonia technologies. Hydrogen is an indirect greenhouse gas with a global warming potential of 11 ±5 over a 100-year time horizon [68]. A study by Derwent at al., in 2006, which has been frequently cited ever since, put the GWP of hydrogen at 5.8.[69]. Leakage can be more prominent in an ammonia plant, however, venting/purging to the environment is not common because they combust these gases to generate heat. Although we did not consider the impact of hydrogen leakage in this study because very little is known about how much hydrogen leaks into the environment from large-scale hydrogen-based plants. However, it is important to comment on the risk of hydrogen leakage to global warming. Hydrogen can contribute to climate change by increasing the lifetime of greenhouse gases such as methane, ozone, and water vapor, resulting in indirect warming. It reacts with tropospheric hydroxyl radicals to perturb the distribution of these greenhouse gases. These tropospheric hydroxyl radicals help to clean up methane emissions. Since methane causes more warming than an equivalent weight of CO_2 over a 20-year period, hydrogen leaks could extend the lifetime of methane in the atmosphere [70]. Therefore, adequate measures must be taken to minimize hydrogen leaks from the synthesis, transportation, and storage to attain a full climate benefit in ammonia production.

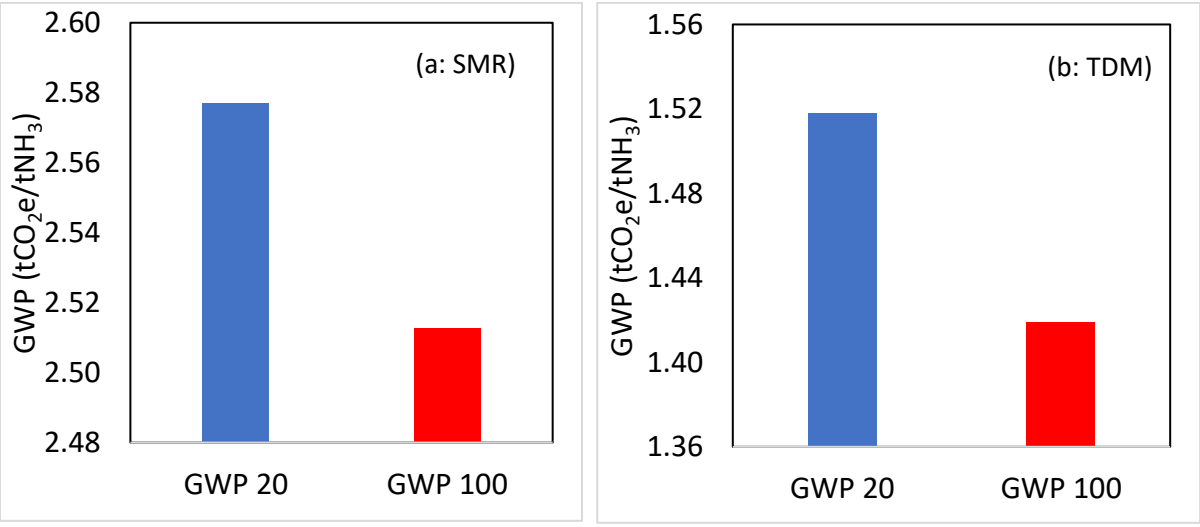

570 Fig. 10: Global warming potential estimates for SMR (a) and TDM (b) using 100-year and 20-year time-
571 horizon

572

573

574 ## 4. Discussion

575 In this section, the potential of the TDM pathway was compared with the SMR pathway. To establish a
576 baseline of understanding, both pathways in terms of their configuration, utilities and raw materials, energy
577 efficiency, greenhouse gas emissions, and economic benefits are discussed.

578 The SMR and TDM pathways comprise different production units to produce ammonia (Fig. 1 and Fig. 2).
579 Only the ammonia synthesis is common to both processes in terms of operation and configuration. The
580 reactor beds and heat exchanger network are practically the same for both pathways. In both pathways, the
581 configuration of each unit minimizes energy use while producing intermediates and final products. The
582 production and treatment of intermediate products (nitrogen and hydrogen) are different for each pathway.
583 SMR needs four reacting stages to achieve the desired hydrogen conversion, whereas TDM needs three.
584 The TDM reactors are more compacted and easily controlled than the SMR reactors. Although both
585 pathways must remove impurities, which are detrimental to the catalyst in the synthesis reactors, steps
586 involved in the SMR pathway are more complex and energy intensive. The SMR pathway requires three
587 purification steps (water separators, CO_2 removal, and methanation). The TDM only needs two (carbon
588 filters and PSA). An air separation unit is inevitable to produce nitrogen in the TDM pathway. In this study,
589 a widely used method of air separation, cryogenic air separation, was adopted. For large-scale production,
590 cryogenic air separation is relatively cheap, and it can produce gases of almost 99.99% purity. The SMR
591 pathway, on the other hand, offers a simplified way to produce nitrogen alongside hydrogen without the
592 use of an ASU.

593 Table 8 presents the utilities and raw materials required to produce 1.0 kg of ammonia for both processes.
594 Other than natural gas feedstock and electricity, the SMR pathway consumes more utilities than the TDM
595 pathway. An example is the heating utility, which is 30.3% higher in SMR. Natural gas consumed as

feedstock in the TDM pathway is 91.7% higher than in the SMR pathway, raising the TDM upstream emissions. Unlike the SMR pathway, the only source of hydrogen for the TDM pathway is natural gas. The SMR pathway consumes lesser natural gas because hydrogen yield stems from both methane and steam. The reaction between methane gas and steam produces hydrogen and carbon monoxide. The carbon monoxide is then shifted with steam to produce CO_2 and more hydrogen in the WGS reactors. One disadvantage of these reaction steps is that it leads to the production of CO_2 emissions. The thermal decomposition of natural gas, however, eliminates CO_2 emissions by producing carbon. Moreover, the carbon product is easy to handle, transport, and cheaper to sequester when compared to CO_2 gas. Increased electricity in the TDM pathway is due to compressions of air in ASU and hydrogen leaving the reactors at a relatively low pressure.

The efficiency of the pathways was evaluated based on the fraction of heat that becomes useful or lost. Because efficiencies of the pathways are in a close range, process performance was assessed using the magnitude of energy losses. The energy loss in the SMR pathway is 1.76 GJ/t NH_3 (22%) higher than in TDM. The energy losses in the pathways are unavoidable because it is necessary to cool streams transiting into another unit.

Regarding the reactors, a substantial part of the overall losses (32.4%) in the TDM pathway is due to unrecovered heat in the stack. Energy loss in the primary reformer is 10% of the overall. The primary reformer appears more energy efficient because it reduces heat load such that flue gas exits the stack with a low energy loss (0.80 GJ/t NH_3). The SMR pathway uses a secondary reformer to reduce the heat load on the primary reformer. Part of the reactions in the primary reformer is shifted to the secondary reformer. The secondary reformer does not require furnace heating. As earlier described, introducing air into the secondary reformer aids the reaction that began in the primary reformer.

The production of nitrogen and purification of intermediate products are important steps for both processes. Compared to air compressions to the SMR reactors, which require 0.48 GJ/t NH_3; in the TDM, producing and compressing nitrogen to the ammonia synthesis reactors require 0.68 GJ/t NH_3. Nitrogen production accounts for 0.32 GJ/t NH_3, which corresponds to 0.375 kWh/kg-O_2. A typical ASU consumes between

622 0.247 and 0.507 kWh/kg-O_2 [71, 72]. For the purification of intermediate products, the SMR pathway is
623 more energy intensive than the TDM pathway, where a PSA unit is employed.
624 Fig. *11* compares the sources of GHG emissions in the SMR and TDM (without CCS). Fuel consumed and
625 process-based emissions make the GHG emissions higher in the SMR. The fuel required to generate heat
626 plays a significant role. The natural gas required for external heating in the primary reformer is about 3.62%
627 higher than in the TDM reactors. When natural gas combustion in the secondary reformer is considered,
628 the percentage increase rises to 48.9%. These increases account for the high GHG emissions in the SMR
629 pathway. The SMR life cycle GHG emission is about 38.8% higher than the TDM pathway. The onsite
630 emissions to the environment take a large share of the life cycle emissions. As earlier mentioned, onsite
631 emissions are an important objective to address. CCS provides a pathway to significantly lower onsite
632 emissions, but it often raises electricity and fossil fuel demand and is expensive. Therefore, it is worth
633 investigating the impact of CCS on both processes. CCS was implemented successfully into the processes,
634 and their performances were evaluated, in section 3 and appendix 2. For the SMR, the process requires two
635 capture points: the purification unit and the primary reformer. Since the process already has MEA scrubber
636 and regenerator, CO_2 emissions are captured by installing compressors, coolers, separators, and storage
637 tanks. To capture emissions from the primary reformer, another MEA scrubber and regenerator to its stack
638 were installed. An additional heat load is needed to meet the regenerator steam demand. This heat load can
639 be provided using a gas-fired heater or the primary reformer. Either way, the additional fuel requirement
640 creates a limitation for a high a high percentage of CO_2 capture in the SMR pathway. However, capturing
641 CO_2 emissions from both points reduces GHG emissions to 1.38 $tCO_2e/t\ NH_3$. The results obtained showed
642 that electricity accounted for 64.5%, upstream 15.9%, combustion emissions 10.8%, and fugitive 8.7%. On
643 the other hand, the TDM pathway requires one capture point, the TDM's furnace. Unlike the SMR, the
644 TDM favors a high percentage of CO_2 capture. Low-pressure steam is generated from the ammonia
645 synthesis unit, thus avoiding the use of a gas-fired heater. Installing the carbon capture unit decreases the
646 base case life cycle GHG emissions to 1.19 $tCO_2e/t\ NH_3$. The electricity, natural gas upstream emissions,
647 combustion emissions, and fugitive emissions account for 60.9%, 32.6%, 4.1% and 2.4%, respectively.

With CCS, the GHG emissions associated with the TDM pathway are lower than the SMR pathway by 14.0%. Although the natural gas upstream emission is high in the TDM, about 75.6% higher than in the SMR, low emissions from combustion, electricity, and fugitives lower the TDM's GHG emissions. It is worth mentioning that fugitive emissions considered for each pathway were assumed to be 7.0% of the transported CO_2 to geological storage. There is limited information on fugitive emissions associated with the transportation and storage of CO_2. About 3-14% of the stored CO_2 escapes based on the limited available literature [73-76]. If we consider this range, the TDM and SMR (with CCS) overall GHG emissions will be 1.17-1.22 $tCO_2e/t\ NH_3$ and 1.31-1.50 $tCO_2e/t\ NH_3$, respectively. The low volume of CO_2 required for transportation using the TDM technology provides an opportunity to lower the overall GHG emissions compared to the SMR technology. Emissions from electricity consumption are also important to be minimized. In both processes, GHG emissions from electricity are high but higher by 8.85% in the TDM pathway. For the base case, the Alberta grid emission factor for 2020 was used, which is a high value because of the high emission intensities of the power sector. Alberta's power sector is currently transitioning from high carbon-based fuels like coal into lesser ones like natural gas and renewables. By 2050, the grid emission factor is likely to reduce by 47.2% by introducing cleaner fuels into the power sector. This reduction can lower the life cycle emissions significantly, but it is a long-term goal. However, running a CHP and biomass-fired power plant is another alternative to lower GHG emissions associated with electricity. For the case without CCS, the use of an energy-efficient natural gas CHP plant with an emission factor of 367 gCO_2e/kWh will lower life cycle GHG emissions by 14.1% (0.20 $tCO_2e/t\ NH_3$) and 8.9% (0.22 $tCO_2e/t\ NH_3$) for TDM and SMR, respectively. By combining a carbon capture unit and a CHP plant, the life cycle GHG emissions are lowered by 32.7% (0.46 $tCO_2e/t\ NH_3$) for TDM and 56.5% (1.42 $tCO_2e/t\ NH_3$) for SMR when compared to the base cases. The application of CCS and CHP positively impacts emissions reduction. Using renewable energy from biomass also offers a reduction in GHG emissions. A biomass-based power plant with an emission factor of 80 gCO_2e/kWh reduces GHG emissions by 37.0% (0.55 $tCO_2e/t\ NH_3$) and 19.2% (0.48 $tCO_2e/t\ NH_3$) for TDM and SMR (cases without CCS),

673 respectively. Although biomass offers a huge environmental benefit to both technologies, its sustainability
674 in terms of costs (capital and operating cost) and availability must be ascertained.
675 Considering the base case scenario, the production cost of ammonia from SMR is lower than TDM by \$69/t
676 NH_3. Without CCS, TDM requires higher investment, and the sale of the oxygen product does not provide
677 sufficient revenue to outperform SMR. TDM (without CCS) needs an oxygen selling price of \$297/t O_2 to
678 compete with the SMR pathway. However, when CCS is integrated into TDM, its economic performance
679 is better. TDM CCS needs an oxygen selling price of \$10/t O_2 to make it competitive with SMR CCS.
680 Based on an oxygen selling price of \$40/t O_2, the cost of ammonia from TDM CCS is \$636/t NH_3, a
681 reduction of 1.1% compared to SMR CCS (\$643/t NH_3). From an economic perspective, the SMR pathway
682 offers a benefit worth spending effort in deployment for ammonia production without integrating a CCS.
683 The decision to implement CCS depends on carbon pricing. The carbon pricing benchmark provides a
684 practical guide for integrating CCS into these processes. CCS is worth implementing when the carbon price
685 is above the production cost because of CCS. Our estimate revealed that SMR (without CCS) is attractive
686 compared to TDM (without CCS) when the carbon pricing benchmark is below \$99/t CO_2. However, at a
687 carbon price above \$99/t CO_2, integrating a CCS into TDM is economically preferable.
688

Table 8: Raw material and utility consumption per kg of ammonia

Material/utility	unit	SMR	TDM
Natural gas feedstock	kg	0.48	0.92
Heating (Fuel)	kg	0.21	0.15
Steam	kg	2.39	0.74
Cooling water	kg	133.92	75.95
Electricity	kWh	1.03	1.13

689

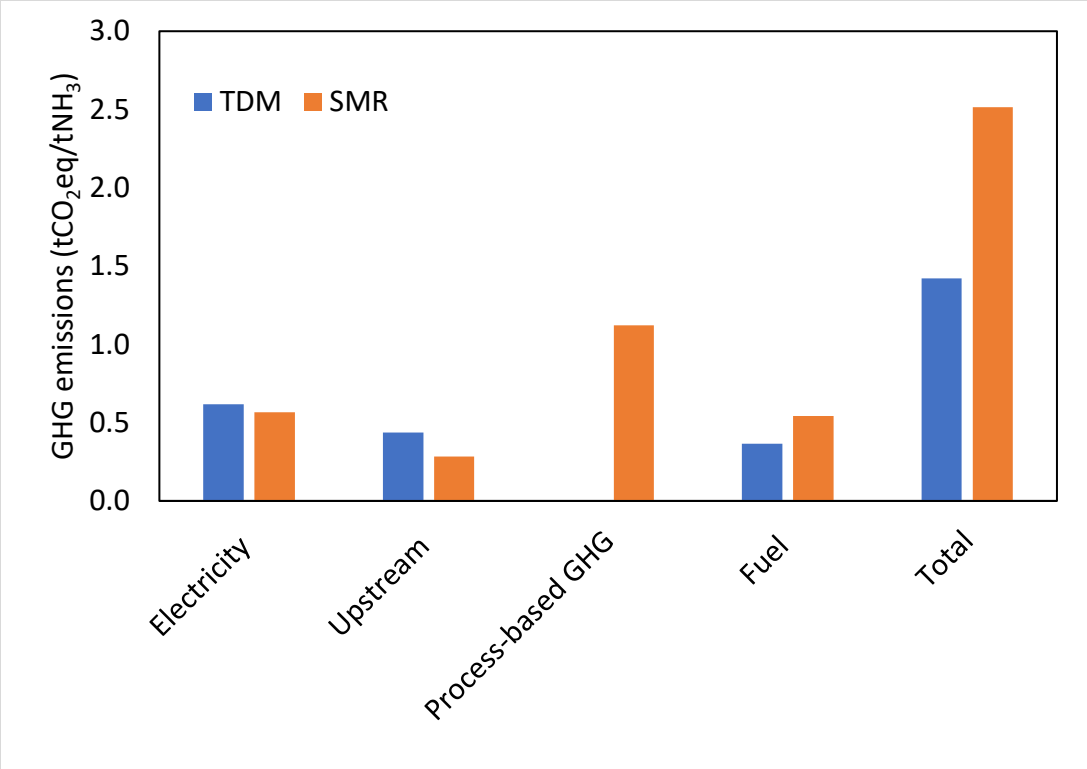

690

691 Fig. 11: Comparing the sources of GHG emissions in the TDM and SMR technologies

692

693 ## 5. Conclusion

694 This study assessed the life cycle greenhouse gas (GHG) and the economic feasibility of applying natural
695 gas decarbonization (TDM) technology for ammonia production compared to the conventional steam
696 methane reforming (SMR) technology. A detailed process model for each ammonia-based technology was
697 developed to obtain data to perform energy, life cycle GHG emissions, and economic analyses. Especially
698 with SMR, where data are available, the results of this work align with values available in the literature.
699 Based on the results of the material and energy analyses, other than natural gas feedstock and electricity,
700 SMR consumes more utilities than TDM. Natural gas consumed as feedstock in TDM is 92.7% higher than
701 in SMR, raising TDM upstream emissions and operating costs. The results also show that the SMR
702 consumes 30.3% more fuel than the TDM. Because efficiencies of the pathways are in a close range, process
703 performance was assessed using the magnitude of energy losses. The magnitude of energy loss in SMR is

22% higher than in TDM. The energy losses in both technologies are unavoidable because it is necessary to cool streams transiting into another unit.

The life cycle GHG emissions of TDM and SMR are 1.42 and 2.51 t CO_2e/t NH_3, respectively. The direct emissions (combustions and process emissions) to the environment and electricity emissions take a large share in the life cycle emissions of SMR and TDM, respectively. The natural gas required to generate heat plays a significant role in the direct emissions. The natural gas required for external heating in the primary reformer (SMR reactor) is about 3.62% higher than in the TDM reactors. When natural gas combustion in the secondary reformer is considered, the percentage increase rises to 48.9%. These increases account for the high GHG emissions in SMR.

Integrating CCS lowers direct emissions significantly but raises electricity, fuel demand, and production cost. Integrating a carbon capture unit and a CHP plant, the life cycle GHG emissions of TDM and SMR were reduced by 35.1% and 69.8%, respectively, compared to using a coal-natural gas mixed electricity grid. The production cost of ammonia from SMR is lower than TDM by \$69/t NH_3. Without CCS, TDM requires higher investment, and the sale of the oxygen product does not provide sufficient revenue to outperform the SMR. However, integrating CCS into TDM improves its economic performance, and it may not require revenue from the sales of an oxygen product.

Regarding the carbon pricing benchmark, CCS is worth implementing when the carbon price is above the production cost because of CCS. Our estimate revealed that SMR (without CCS) is more economically attractive when the carbon price benchmark is below \$99/t CO_2. At a carbon price above \$99/t CO_2, integrating a CCS into TDM is economically preferable.

Lastly, the air separation unit contributes significantly to the production cost of ammonia in TDM. There might be great potential for an alternative that replaces the air separation unit with a lower impact on the production cost of ammonia. Future work will investigate the potential of reducing the investment in TDM by replacing the air separation unit with an economical alternative. Providing nitrogen through an autothermal reactor (secondary reformer) and/or from a gas power plant (exhaust flue gas) instead of using ASU is ongoing work.

6. Appendix

Appendix A1 [77, 78]

Ammonia synthesis process

$N_2 + 3H_2 \leftrightarrow 2NH_3 \qquad \Delta H_{298K} = -92.44\ kJ/mol$ *(1)*

$k_1 = 1.79 \times 10^4 e^{-87{,}090/RT}$ *(2)*

$k_2 = 2.75 \times 10^{16} e^{-198{,}464/RT}$ *(3)*

Steam methane reforming reactions in the primary reactor

$CH_4 + H_2O \leftrightarrow CO + 3H_2 \qquad \Delta H_{298K} = 205.8\ kJ/mol$ *(4)*

$k_{1023K} = 47.67$, $k_{1073K} = 164.1$, and $k_{1123K} = 507.59$

$CH_4 + 2H_2O \leftrightarrow CO_2 + 4H_2 \qquad \Delta H_{298K} = 164.65\ kJ/mol$ *(5)*

$K_{1023K} = 63.41$, $k_{1073K} = 181.1$, and $k_{1123K} = 473.37$

Authothemal reforming reactions in the secondary reactor

$CH_4 + 0.5O_2 = CO + 2H_2 \qquad \Delta H_{298K} = -36\ kJ/mol$ *(6)*

$K_{1023K} = 2.8 \times 10^{11}$, $k_{1073K} = 2.5 \times 10^{11}$, and $k_{1123K} = 2.2 \times 10^{11}$

$CH_4 + 2H_2O \leftrightarrow CO_2 + 4H_2 \qquad \Delta H_{298K} = 164.65\ kJ/mol$ *(7)*

$K_{1023K} = 63.41$, $k_{1073K} = 181.1$, and $k_{1123K} = 473.37$

$CH_4 + O_2 \leftrightarrow CO_2 + 2H_2 \qquad \Delta H_{298K} = -318.99\ kJ/mol$ *(8)*

$K_{1023K} = 2.2 \times 10^{21}$, $k_{1073K} = 4.1 \times 10^{21}$, and $k_{1123K} = 8.9 \times 10^{19}$

$CH_4 = C + 2H_2 \qquad \Delta H_{298K} = 74.52\ kJ/mol$ *(9)*

$k_{1023K} = 13.12$, $k_{1073K} = 21.42$, and $k_{1123K} = 33.54$

$C + O_2 = CO_2$ $\Delta H_{298K} = -393.51\ kJ/mol$ *(10)*

$K_{1023K} = 1.6 \times 10^{20}$, $k_{1073K} = 1.9 \times 10^{19}$, *and* $k_{1123K} = 6.6 \times 10^{9}$

Water gas shift reaction

$CO + H_2O \leftrightarrow CO_2 + H_2$ $\Delta H_{298K} = -41.17\ kJ/mol$ *(8)*

$k_{1023K} = 1.33$, $k_{1073K} = 1.1$, *and* $k_{1123K} = 0.93$

Methane decomposition reaction

$CH_4 = C + 2H_2$ $\Delta H_{298K} = 74.52\ kJ/mol$ *(9)*

$k_{1023K} = 13.12$, $k_{1073K} = 21.42$, *and* $k_{1123K} = 33.54$

Appendix A2

Table A1: Economic breakdown of ammonia production cost with and without CCS

	SMR		TDM	
	Without CCS	With CCS	Without CCS	With CCS
Production cost ($/tonne)	500	643	569	645
CAPEX ($M)	807	944	946	1,029
COM ($M/year)	400	451	382	440

7. References

1. U.S. Geological Survey. Nitrogen (Fixed) - Ammonia Statistics. 2016 [cited 2021 February]; Available from: https://www.usgs.gov/centers/nmic/nitrogen-statistics-and-information.
2. Statista. Chemicals & Resources - Statistics and facts on chemicals and resources. 2021 [cited 2021 February]; Available from: https://www.statista.com/statistics/1065865/ammonia-production-capacity-globally/.
3. Liu H, Ammonia synthesis catalyst 100 years: Practice, enlightenment and challenge. Chinese journal of catalysis, 2014. **35**(10): p. 1619-1640.
4. Giddey S, Badwal S, Munnings C, and Dolan M, Ammonia as a renewable energy transportation media. ACS Sustainable Chemistry & Engineering, 2017. **5**(11): p. 10231-10239.
5. Pattabathula, V. and J. Richardson, Introduction to ammonia production. Chem. Eng. Prog, 2016. **112**: p. 69-75.
6. Malins C. What role for electromethane and electroammonia technologies in European transport's low carbon future? 2018 [cited 2020 March 1]; Available from: https://www.transportenvironment.org/sites/te/files/publications/2018_06_Cerulogy_What-role-electromethane-and-electroammonia_June2018.pdf.
7. Industrial Efficiency Technology Database. The Institute for Industrial Productivity (IIP). 2015 [cited 2021 March 1]; Available from: http://www.iipinetwork.org/resources/industrial-efficiency-technology-database.
8. Natural Resources Canada (NRC), Canadian Ammonia Producers: Benchmarking Energy Efficiency and Carbon Dioxide Emissions. 2007, Ottawa: Canadian Industry Program for Energy Conservation, Ottawa.
9. Feeding the Earth. Energy Efficiency and CO2 emissions in ammonia production. 2009 [cited 2021 March 1]; Available from: https://www.fertilizer.org/images/Library_Downloads/2009_IFA_energy_efficiency.pdf.
10. Liu X, Elgowainy A, and Wang M, Life cycle energy use and greenhouse gas emissions of ammonia production from renewable resources and industrial by-products. Green Chemistry, 2020. **22**(17): p. 5751-5761.
11. Zhang, W.-f., Z.-x. Dou, P. He, X.-T. Ju, D. Powlson, D. Chadwick, D. Norse, Y.-L. Lu, Y. Zhang, and L. Wu, New technologies reduce greenhouse gas emissions from nitrogenous fertilizer in China. Proceedings of the National Academy of Sciences, 2013. **110**(21): p. 8375-8380.
12. Kahrl, F., Y. Li, Y. Su, T. Tennigkeit, A. Wilkes, and J. Xu, Greenhouse gas emissions from nitrogen fertilizer use in China. Environmental science & policy, 2010. **13**(8): p. 688-694.
13. Zhang, H., L. Wang, F. Maréchal, and U. Desideri, Techno-economic comparison of green ammonia production processes. Applied Energy, 2020. **259**: p. 114135.
14. Bicer Y, Dincer I, Vezina G, and Raso F, Impact assessment and environmental evaluation of various ammonia production processes. Environmental management, 2017. **59**(5): p. 842-855.
15. Kumar, A., S. Adamopoulos, D. Jones, and S.O. Amiandamhen, Forest biomass availability and utilization potential in Sweden: A review. Waste and Biomass Valorization, 2020: p. 1-16.
16. Milbrandt, A. and R.P. Overend. Survey of biomass resource assessments and assessment capabilities in APEC economies. 2008 [cited 2020 March 1]; Available from: https://www.nrel.gov/docs/fy09osti/43710.pdf.
17. Wiedinmyer, C., R.J. Yokelson, and B.K. Gullett, Global emissions of trace gases, particulate matter, and hazardous air pollutants from open burning of domestic waste. Environmental science & technology, 2014. **48**(16): p. 9523-9530.

18. Cheng K, Hao W, Wang Y, Yi P, Zhang J, and Ji W, Understanding the emission pattern and source contribution of hazardous air pollutants from open burning of municipal solid waste in China. Environmental Pollution, 2020. **263**: p. 114417.
19. Weger, L., A. Abánades, and T. Butler, Methane cracking as a bridge technology to the hydrogen economy. international journal of hydrogen energy, 2017. **42**(1): p. 720-731.
20. Abánades A, Natural gas decarbonization as tool for Greenhouse Gases Emission Control. Frontiers in Energy Research, 2018. **6**: p. 47.
21. Keipi, T., V. Hankalin, J. Nummelin, and R. Raiko, Techno-economic analysis of four concepts for thermal decomposition of methane: reduction of CO2 emissions in natural gas combustion. Energy Conversion and Management, 2016. **110**: p. 1-12.
22. Keipi, T., H. Tolvanen, and J. Konttinen, Economic analysis of hydrogen production by methane thermal decomposition: Comparison to competing technologies. Energy Conversion and Management, 2018. **159**: p. 264-273.
23. Nduagu, E. and I. Gates, Process analysis of a low emissions hydrogen and steam generation technology for oil sands operations. Applied Energy, 2015. **146**: p. 184-195.
24. Nduagu, E. and I. Gates, Economic assessment of natural gas decarbonization technology for carbon emissions reduction of bitumen recovery from oil sands. International Journal of Greenhouse Gas Control, 2016. **55**: p. 153-165.
25. Appl M, Ammonia, 3. Production Plants. Ullmann's Encyclopedia of Industrial Chemistry, 2000.
26. Appl M, Ammonia: Priciples & Industrial Practice. 1999, Federal Republic of Germany: Wiley-VCH
27. Aaron D and Tsouris C, Separation of CO2 from flue gas: a review. Separation science and technology, 2005. **40**(1-3): p. 321-348.
28. Xue B, Yu Y, Chen J, Luo X, and Wang M, A comparative study of MEA and DEA for post-combustion CO2 capture with different process configurations. International Journal of Coal Science & Technology, 2017. **4**(1): p. 15-24.
29. Spath P.L and Mann M.K., Biomass power and conventional fossil systems with and without CO2 sequestration-comparing the energy balance, greenhouse gas emissions and economics. 2004, EERE Publication and Product Library, Washington, DC (United States).
30. Luis P, Use of monoethanolamine (MEA) for CO2 capture in a global scenario: Consequences and alternatives. Desalination, 2016. **380**: p. 93-99.
31. Parkash, S., Refining processes handbook. 2003: Elsevier.
32. ISO International organization for standardization, ISO 14040:2006 Environmental management–life cycle assessment–principles and framework 2006-07.
33. ISO International Organization for Standardization, ISO 14044:2006 Environmental management -- Life cycle assessment -- Requirements and guidelines. 2006-07.
34. The Intergovernmental Panel on Climate Change. IPCC AR6 - Climate Change 2021, The Physical Science Basis - Chapter 7. 2022 [cited 2022 September 1]; Available from: https://www.ipcc.ch/report/sixth-assessment-report-working-group-i/.
35. Canada Energy Regulator. Canada's energy future 2020: Canada's energy supply and demand projections to 2050. 2020 [cited 2022 September 1]; Available from: https://www.cer-rec.gc.ca/en/data-analysis/canada-energy-future/2020/index.html.
36. Environment and Climate Change Canada. National inventory report 1990e2018: greenhouse gas sources and sinks in Canada. 2020 [cited 2022 September 1]; Available from: https://publications.gc.ca/collections/collection_2020/eccc/En81-4-1-2018-eng.pdf.
37. Salkuyeh Y.K, Saville B.A, and MacLean H.L, Techno-economic analysis and life cycle assessment of hydrogen production from natural gas using current and emerging technologies. International Journal of hydrogen energy, 2017. **42**(30): p. 18894-18909.
38. Bartels J.R, A feasibility study of implementing an Ammonia Economy. 2008, Iowa State University.

855 39. Lane J and Spath P, Technoeconomic analysis of the thermocatalytic decomposition of natural
856 gas. 2001, National Renewable Energy Lab., Golden, CO (US).
857 40. Larson E.D, Jin H, and Celik F.E, Large-scale gasification-based coproduction of fuels and electricity
858 from switchgrass. Biofuels, Bioproducts and Biorefining, 2009. **3**(2): p. 174-194.
859 41. Kreutz, T., R. Williams, S. Consonni, and P. Chiesa, Co-production of hydrogen, electricity and CO2
860 from coal with commercially ready technology. Part B: Economic analysis. International Journal of
861 Hydrogen Energy, 2005. **30**(7): p. 769-784.
862 42. Turton, R., R.C. Bailie, W.B. Whiting, and J.A. Shaeiwitz, Analysis, synthesis and design of chemical
863 processes. 2008: Pearson Education.
864 43. GREET, Model 4.02 a. Argonne National Laboratory, US Department of Energy, 2012.
865 44. Siegl S, Laaber M, and Holubar P, Green electricity from biomass, part I: Environmental impacts
866 of direct life cycle emissions. Waste and Biomass Valorization, 2011. **2**(3): p. 267-284.
867 45. Oni, A., K. Anaya, T. Giwa, G. Di Lullo, and A. Kumar, Comparative assessment of blue hydrogen
868 from steam methane reforming, autothermal reforming, and natural gas decomposition
869 technologies for natural gas-producing regions. Energy Conversion and Management, 2022. **254**:
870 p. 115245.
871 46. Herzog H, Smekens K, D. P., Dooley J, Fujii Y, Hohmeyer O, and Riahi K. Cost and economic
872 potential. 2005 [cited 2021 March 20]; Available from:
873 https://www.ipcc.ch/site/assets/uploads/2018/03/srccs_chapter8-1.pdf.
874 47. Peters, M.S., K.D. Timmerhaus, and R.E. West, Plant design and economics for chemical engineers.
875 Vol. 4. 2003: McGraw-Hill New York.
876 48. Bañares-Alcántara R, Dericks IIIG, Fiaschetti M, Grünewald P, Lopez J.M, E. Tsang , Yang A, Ye L,
877 and Zhao S, Analysis of islanded ammonia-based energy storage systems. University of Oxford,
878 2015.
879 49. Insider. Markets Insider. 2020 [cited 2020 July]; Available from:
880 https://markets.businessinsider.com/commodities/iron-ore-price.
881 50. Oko, E., B. Zacchello, M. Wang, and A. Fethi, Process analysis and economic evaluation of mixed
882 aqueous ionic liquid and monoethanolamine (MEA) solvent for CO2 capture from a coke oven
883 plant. Greenhouse Gases: Science and Technology, 2018. **8**(4): p. 686-700.
884 51. Dorris C.C, Lu E, Park S, and Toro F.H, High-purity oxygen production using mixed ionic-electronic
885 conducting sorbents. 2016.
886 52. Andersson J and Lundgren J, Techno-economic analysis of ammonia production via integrated
887 biomass gasification. Applied Energy, 2014. **130**: p. 484-490.
888 53. McVickar, M., W. Martin, I.E. Miles, and H. Tucker, Agricultural anhydrous ammonia, technology
889 and use. Agricultural anhydrous ammonia, technology and use., 1966.
890 54. Smith, C., A.K. Hill, and L. Torrente-Murciano, Current and future role of Haber–Bosch ammonia
891 in a carbon-free energy landscape. Energy & Environmental Science, 2020. **13**(2): p. 331-344.
892 55. Natural Resources Canada (NRC) and Canadian Ammonia Producer, Benchmarking Energy
893 Efficiency and Carbon Dioxide Emissions. 2008, Natural Resources Canada, Ottawa, Canada.
894 56. Appl M, Ammonia. Ullmann's Encyclopedia of Industrial Chemistry, 2000.
895 57. Rutkowski, M. Current (2005) hydrogen from SMR natural gas with CO2 capture and
896 sequestration. 2005 [cited 2008 March]; Available from:
897 http://www.hydrogen.energy.gov/h2a_prod_studies.html.
898 58. Suelves, I., M. Lázaro, R. Moliner, B. Corbella, and J. Palacios, Hydrogen production by thermo
899 catalytic decomposition of methane on Ni-based catalysts: influence of operating conditions on
900 catalyst deactivation and carbon characteristics. International Journal of Hydrogen Energy, 2005.
901 **30**(15): p. 1555-1567.

59. Steinberg, M., Fossil fuel decarbonization technology for mitigating global warming. International Journal of Hydrogen Energy, 1999. **24**(8): p. 771-777.
60. Sánchez-Bastardo, N., R. Schlögl, and H. Ruland, Methane Pyrolysis for CO2-Free H2 Production: A Green Process to Overcome Renewable Energies Unsteadiness. Chemie Ingenieur Technik, 2020. **92**(10): p. 1596-1609.
61. Amin A.M, Croiset E, Malaibari Z, and Epling W, Hydrogen production by methane cracking using Ni-supported catalysts in a fluidized bed. international journal of hydrogen energy, 2012. **37**(14): p. 10690-10701.
62. Aiello R, Fiscus J.E, Zur L.H, and Amiridis M.D, Hydrogen production via the direct cracking of methane over Ni/SiO2: catalyst deactivation and regeneration. Applied Catalysis A: General, 2000. **192**(2): p. 227-234.
63. Shah, N., S. Ma, Y. Wang, and G.P. Huffman, Semi-continuous hydrogen production from catalytic methane decomposition using a fluidized-bed reactor. International journal of hydrogen energy, 2007. **32**(15): p. 3315-3319.
64. Henriksson P.J.G, Heijungs R, Dao H.M, Phan L.T, de Snoo G.R, and Guinée J.B, Product carbon footprints and their uncertainties in comparative decision contexts. PloS one, 2015. **10**(3): p. e0121221.
65. MacKay K, Lavoie M, Bourlon E, Atherton E, O'Connell E, Baillie J, Fougère C, and Risk D, Methane emissions from upstream oil and gas production in Canada are underestimated. Scientific reports, 2021. **11**(1): p. 1-8.
66. Di Lullo G, Zhang H, and Kumar A, Evaluation of uncertainty in the well-to-tank and combustion greenhouse gas emissions of various transportation fuels. Applied energy, 2016. **184**: p. 413-426.
67. Di Lullo G, Oni A.O, Gemechu E, and Kumar A, Developing a greenhouse gas life cycle assessment framework for natural gas transmission pipelines. Journal of Natural Gas Science and Engineering, 2020. **75**: p. 103136.
68. Frazer-Nash Consultancy. Fugitive Hydrogen Emissions in a Future Hydrogen Economy, Department for Business, Energy & Industrial Strategy. 2022 [cited 2022 September 1]; Available from: https://assets.publishing.service.gov.uk/government/uploads/system/uploads/attachment_data/file/1067137/fugitive-hydrogen-emissions-future-hydrogen-economy.pdf.
69. Derwent R, Simmonds P, O Doherty S, Manning A, Collins W, and Stevenson D, Global environmental impacts of the hydrogen economy. International Journal of Nuclear Hydrogen Production and Applications, 2006. **1**(1): p. 57.
70. Warwick N, Griffiths P, Keeble J, Archibald A, Pyle J, and Shine K. Atmospheric implications of increased Hydrogen use. AvaliableAt: https://assets. publishing. service. gov. uk/government/uploads/system/uploads/attachment_data/file/1067144/atmospheric-implications-of-increased-hydrogen-use. pdf 2022 [cited 2022 September 1]; 75]. Available from: https://assets.publishing.service.gov.uk/government/uploads/system/uploads/attachment_data/file/1067144/atmospheric-implications-of-increased-hydrogen-use.pdf.
71. DOE/NETL. Pulverized coal oxycombustion Power Plants, Volume 1: bituminous coal to electricity, report DOE/NETL-2007/1291. National Energy Technology Laboratory 2007 [cited 2021 March 1]; Available from: http://www.netl.doe.gov/energy-analyses/pubs/PC%20Oxyfuel%20Combustion%20Revised%20Report%202008.pdf.
72. Netzer, D. Alberta bitumen processing integration study final report. Report prepared for the Province of Alberta Economic Development Department and the Alberta Energy Research Institute (March 2006) 2006 [cited 2021 April 1]; Available from: https://open.alberta.ca/dataset/7d728b7f-e97c-4c01-ba2a-b527399b40fa/resource/127b6abd-47d0-496f-9cc8-338bf9e9f032/download/albertabitumenprocessintegrationreport06.pdf.

73. Beaubien S.E, Jones D.G, Gal F, Barkwith A, Braibant G, Baubron J-C, Ciotoli G, Graziani S, Lister TR, and Lombardi S, Monitoring of near-surface gas geochemistry at the Weyburn, Canada, CO2-EOR site, 2001–2011. International Journal of Greenhouse Gas Control, 2013. **16**: p. S236-S262.
74. Guangzhong L, Zhenquan L, and Xiangliang L, Technology and application of CO2 capture, utilization and storage for coalfired power plant. Science & Technology Review, 2014. **32**(1): p. 40-45.
75. Zhang L, Huang H, Wang Y, Ren B, Ren S, Chen G, and Zhang H, CO2 storage safety and leakage monitoring in the CCS demonstration project of Jilin oilfield, China. Greenhouse Gases: Science and Technology, 2014. **4**(4): p. 425-439.
76. Yang Y, Li Y, Zhang S, Chen F, Hou H, and Ma J, Monitoring the impact of fugitive CO2 emissions on wheat growth in CCS-EOR areas using satellite and field data. Journal of Cleaner Production, 2017. **151**: p. 34-42.
77. Morud, J.C. and S. Skogestad, Analysis of instability in an industrial ammonia reactor. AIChE Journal, 1998. **44**(4): p. 888-895.
78. Souza, A.E., L.J. Maciel, V.O. Cavalcanti-Filho, N.M.L. Filho, and C.A. Abreu, Kinetic-operational mechanism to autothermal reforming of methane. Industrial & engineering chemistry research, 2011. **50**(5): p. 2585-2599.